

About my last master semester...

- In October 2013 I moved to **Rotterdam**, the Netherlands
- Erasmus University Medical Center (Erasmus MC)
- Biomedical Imaging Group Rotterdam (BIGR)
Head: Prof. Wiro Niessen
- Supervisors FAU: Stefan Steidl, Andreas Maier
- Supervisors BIGR: Adria Perez-Rovira, Marleen de Bruijne



Characterization of Lung Motion in Pompe Patients using 3D+t MRI Data

Thesis presentation

Katja Mogalle

June 30, 2014

Computer Science Dept. 5 (Pattern Recognition)

Friedrich-Alexander-Universität Erlangen-Nürnberg



Outline

- Introduction
- The Big Picture
- Bias Field Correction
- Respiratory Motion Estimation
- Lung Surface Partitioning
- Motion Feature Extraction
- Conclusion and Outlook

Pompe Disease

Rare inherited metabolic disorder

- 1 in 40.000 affected
- reduced activity of enzyme α -glucosidase
- glycogen accumulates and damages muscles

Symptoms

- slowly progressive myopathy
- wheelchair and/or ventilator dependency
- high variety in age of onset and course of disease

Treatment (Enzyme Replacement Therapy)

- very expensive
- highest success rate for patients at **early** disease stage

Motivation

Respiratory failure is major cause of death (monitored with spirometry)

Involvement of diaphragm must be detected early

Magnetic Resonance Imaging

- non-invasive
- advanced protocols allow for **dynamic 3D imaging** of thorax during breathing

Goal

- analyze breathing mechanics
- assess functioning of diaphragm

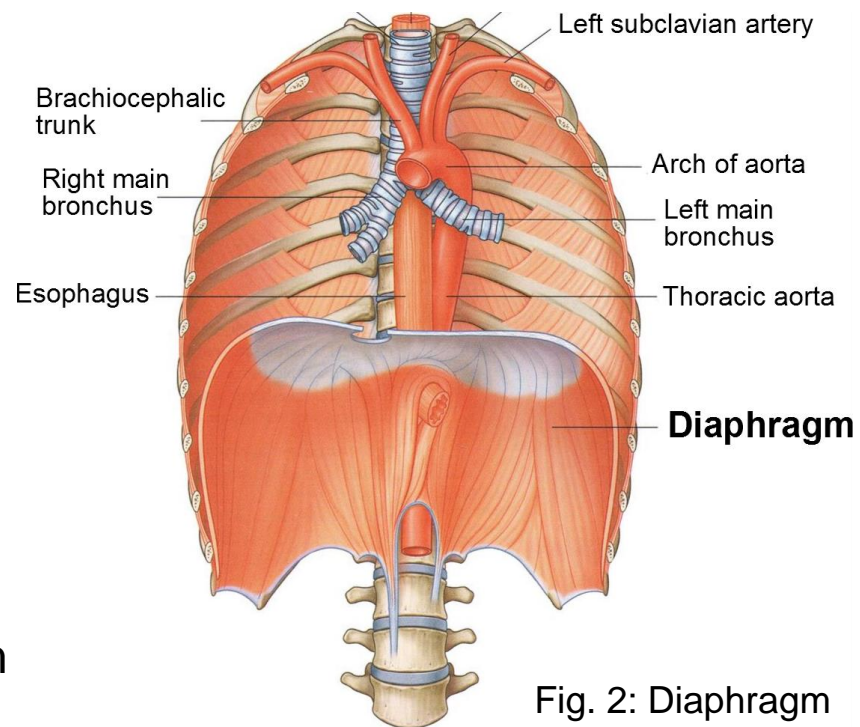
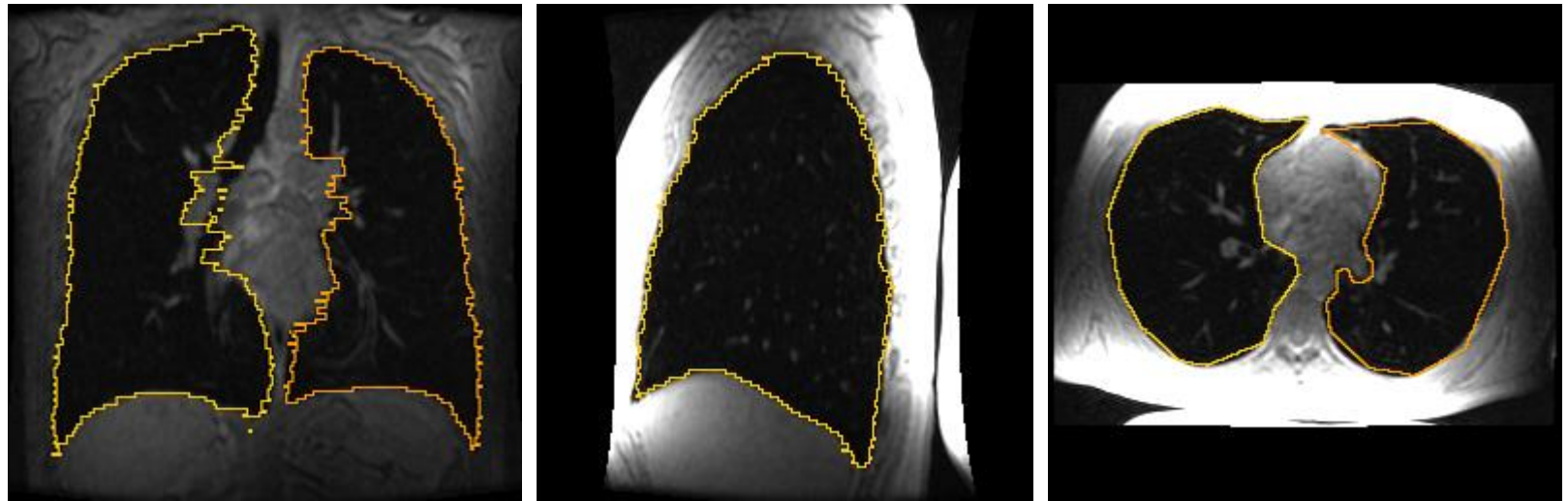


Fig. 2: Diaphragm

Data

MRI images for 10 Pompe patients and 6 healthy volunteers

- 3D static scan at end inspiration and manual lung segmentation

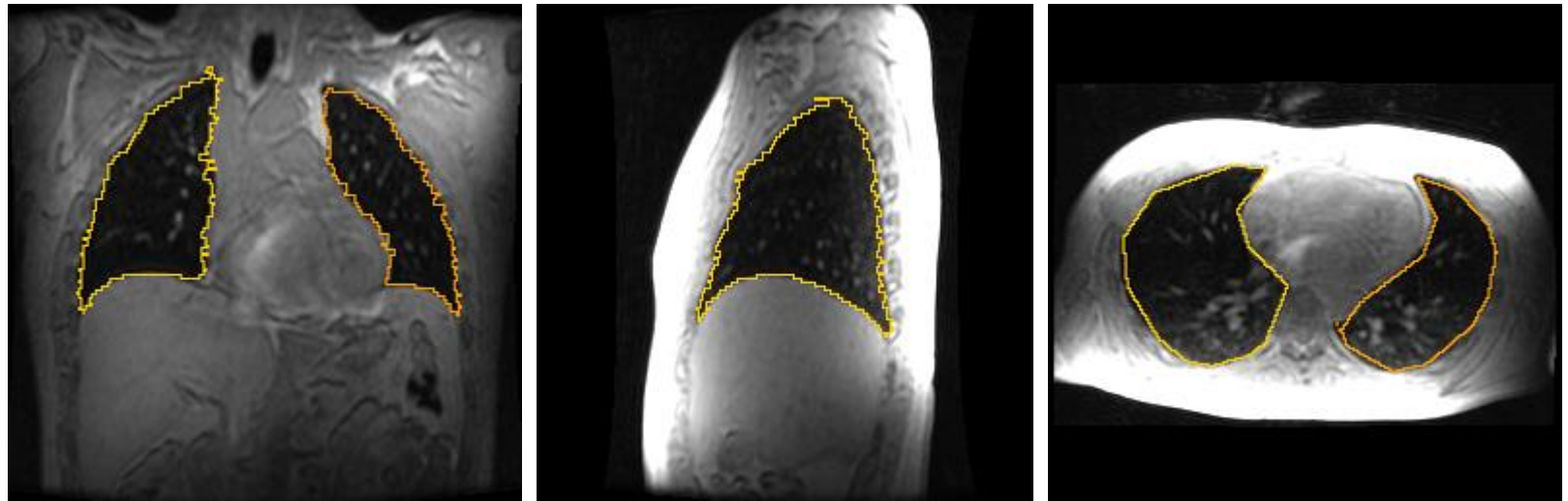


Volunteer 04, dimensions: 256 x 256 x 248, voxel size 1.46 x 1.46 x 1.5 mm

Data

MRI images for 10 Pompe patients and 6 healthy volunteers

- 3D static scan at end expiration and manual lung segmentation

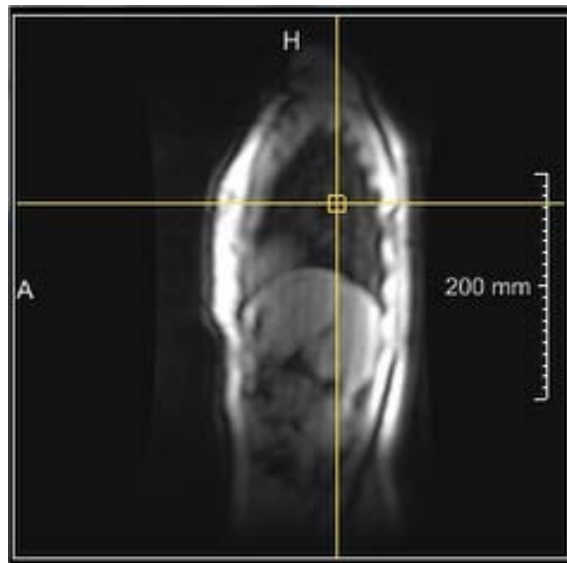


Volunteer 04, dimensions: 256 x 256 x 248, voxel size 1.46 x 1.46 x 1.5 mm

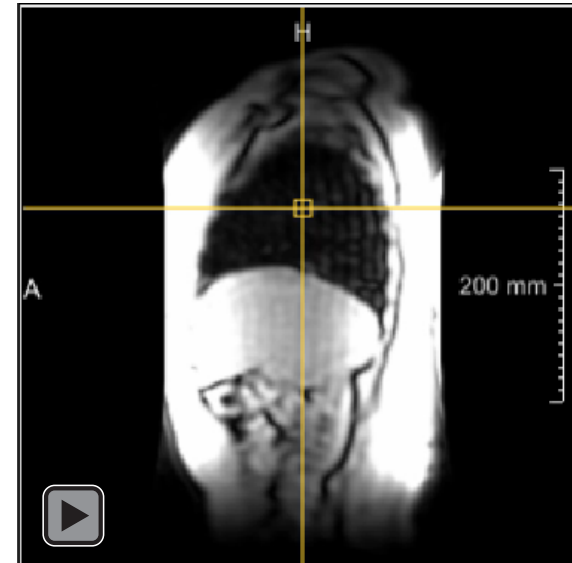
Data

MRI images for 10 Pompe patients and 6 healthy volunteers

- 3D+t **dynamic scan** (256x256x60x48 voxels, voxel size 1.875x1.875x6 mm)



Volunteer 03



Patient 07

State of the Art

- 62.5% [Kondo 2000] – 75% [Naish 2009] of the **lung volume change** is induced by **diaphragmatic movement**

State of the Art

- 62.5% [Kondo 2000] – 75% [Naish 2009] of the **lung volume change** is induced by **diaphragmatic movement**
- lung volume measurements in MRI data correlate well with spirometry data, further analysis on normal diaphragm shape and movement [Gauthier 1994]

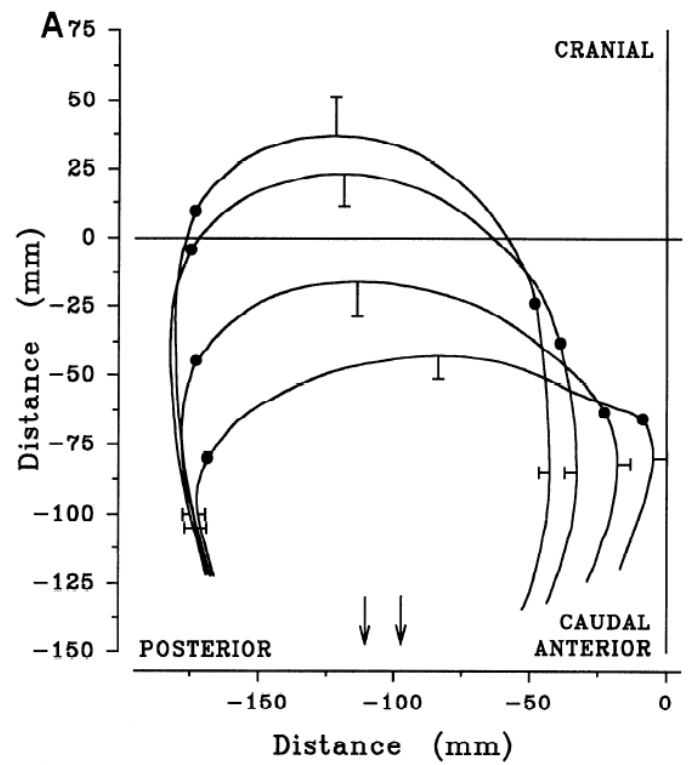


Fig. 4: Diaphragm movement

State of the Art

- 62.5% [Kondo 2000] – 75% [Naish 2009] of the **lung volume change** is induced by **diaphragmatic movement**
- lung volume measurements in MRI data correlate well with spirometry data, further analysis on normal diaphragm shape and movement [Gauthier 1994]
- lung motion estimation in 3D+t MRI data [Plathow 2009] via statistical shape models and active shape mechanism [Heimann 2007], to analyze impact of lung tumors

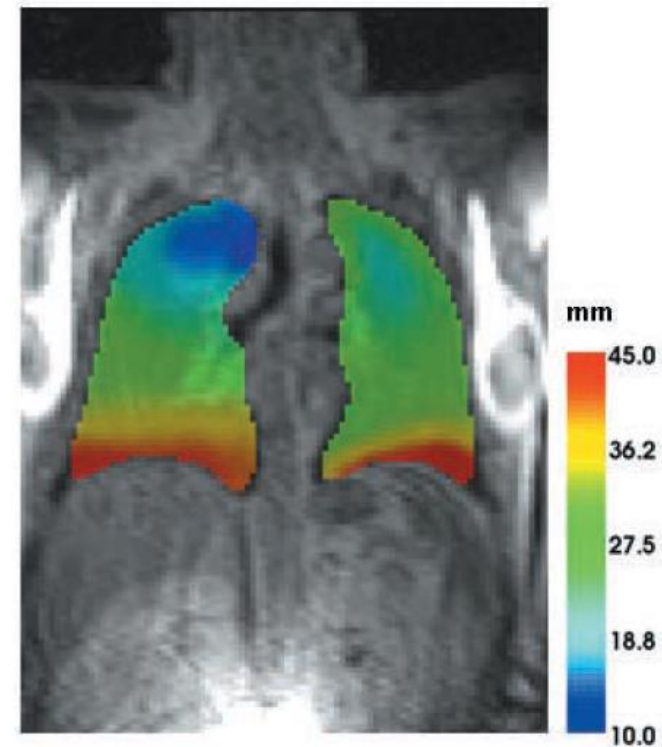
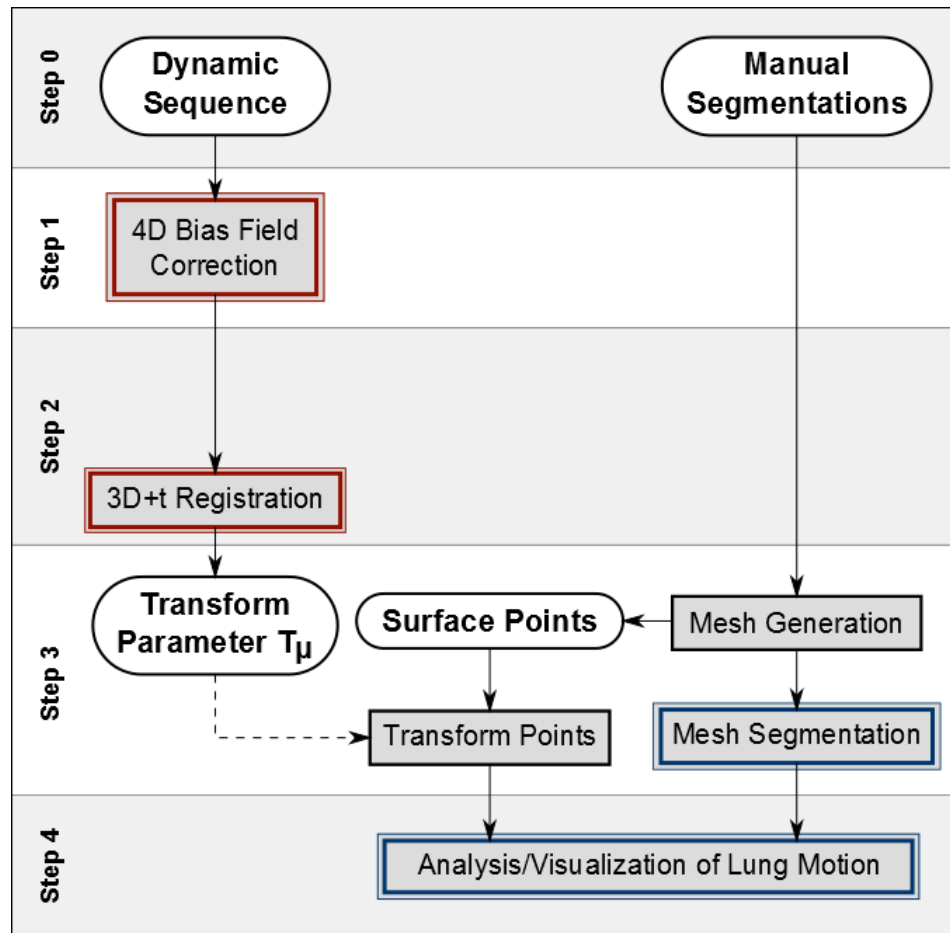
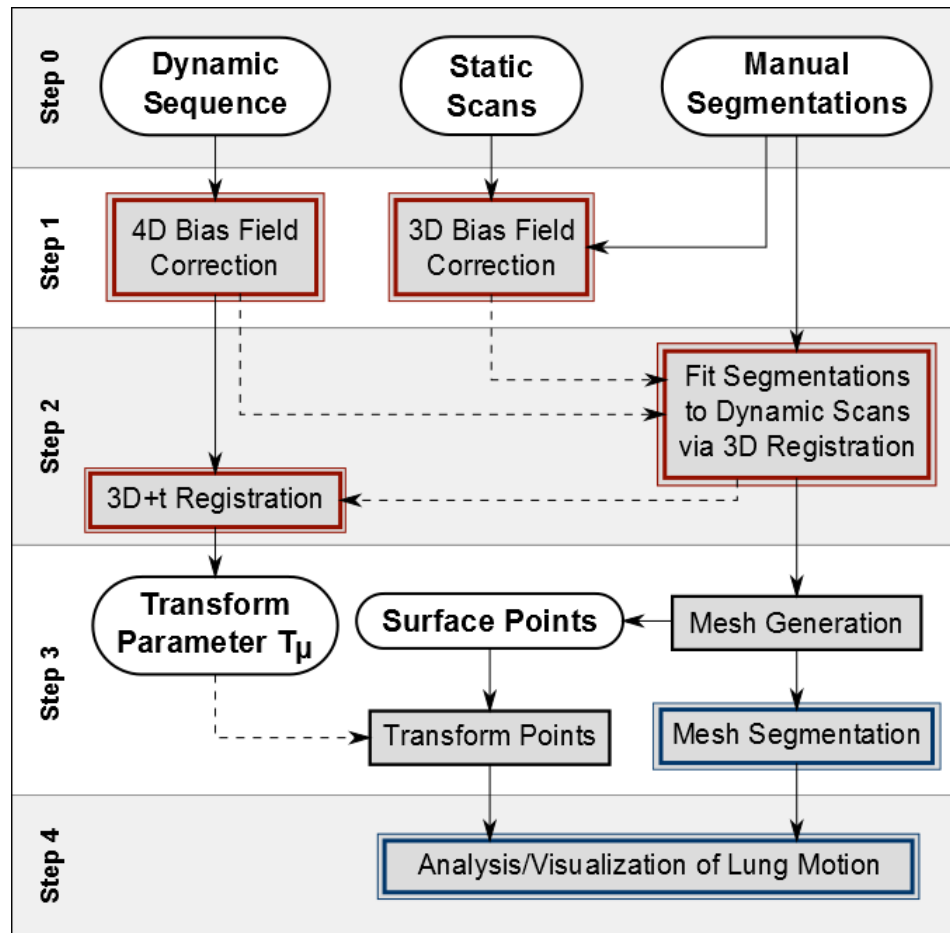


Fig. 5: Lung deformation

Pipeline

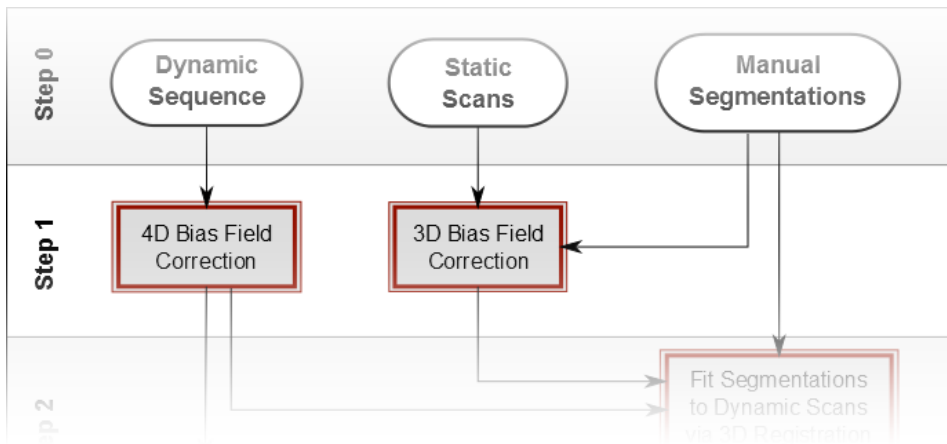


Pipeline





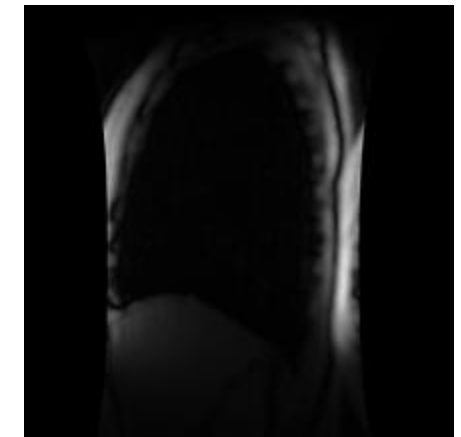
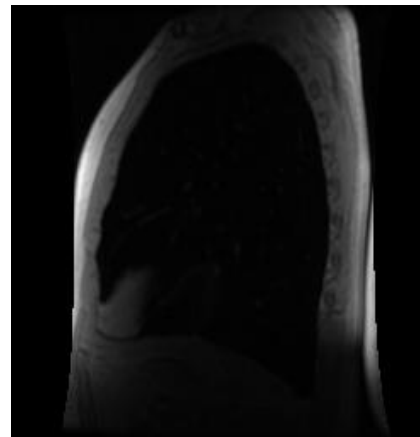
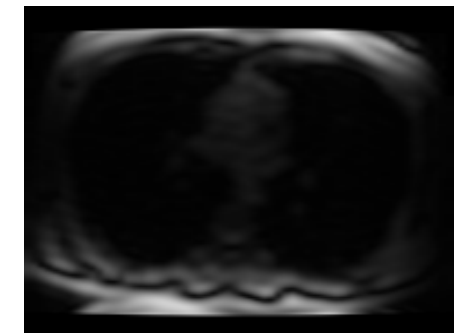
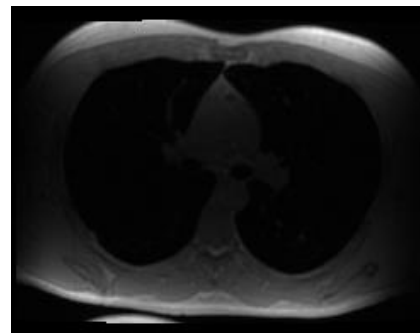
Bias Field Correction



Intensity Inhomogeneity

Possible reasons for intensity inhomogeneity

- surface coil sensitivity
- fat/water contrast



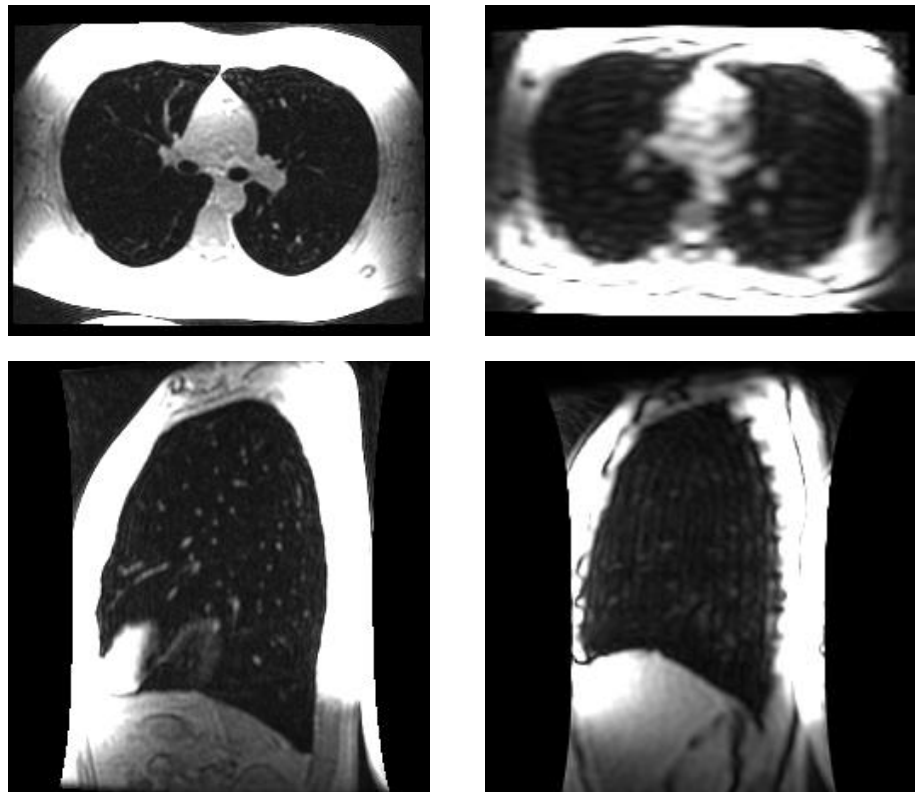
Intensity Inhomogeneity

Possible reasons for intensity inhomogeneity

- surface coil sensitivity
- fat/water contrast

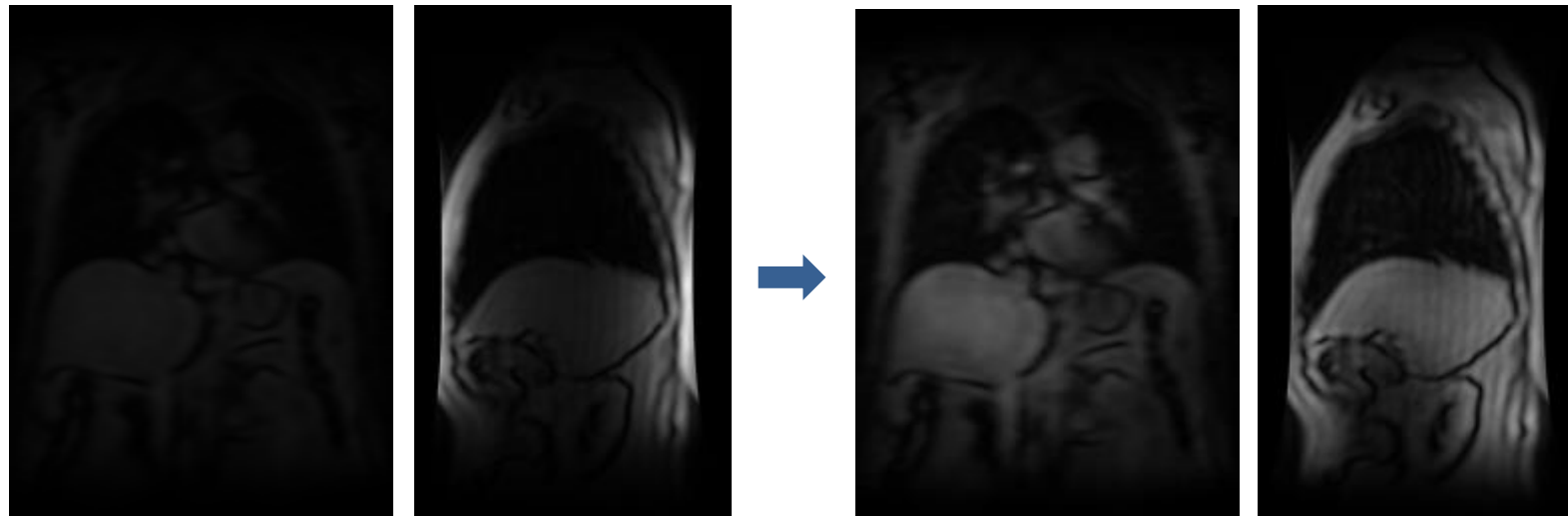
→ manual contrast adjustment shows inner structures

Bias field correction necessary for succeeding registration



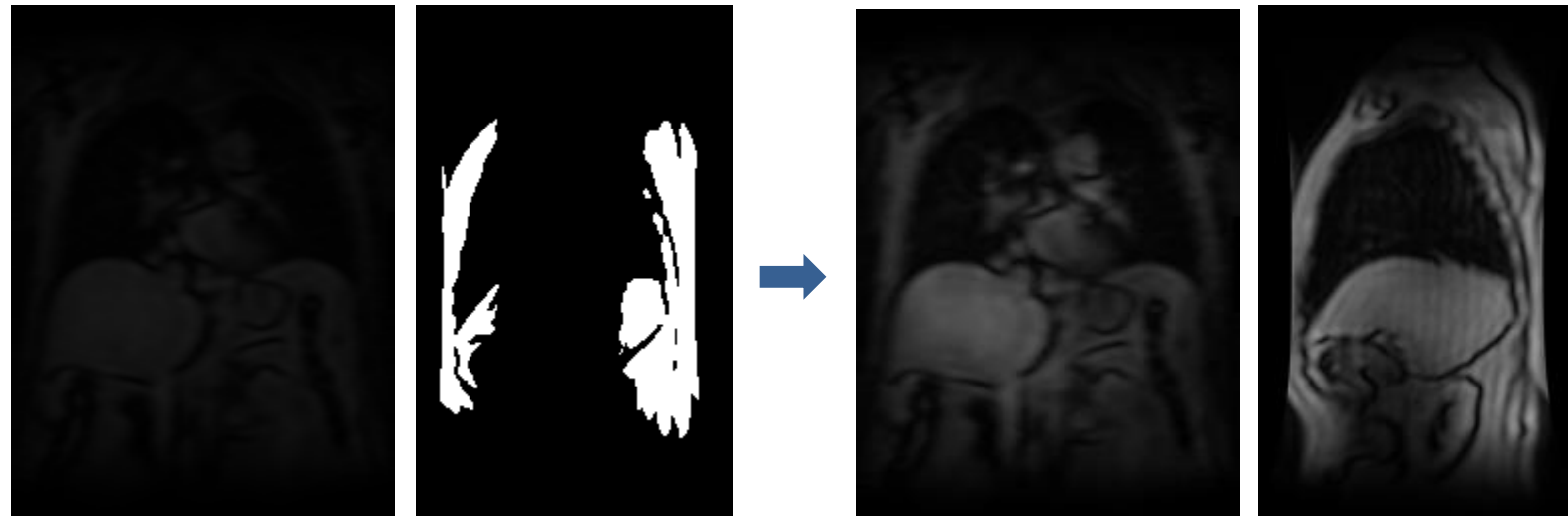
Bias Field Correction with N4ITK [Tustison 2010]

- extension of popular N3 algorithm [Sled 1998]
- iterative method for bias field estimation using:
 - B-spline approximation
 - multi-resolution
 - masks, weight image



Bias Field Correction with N4ITK [Tustison 2010]

- extension of popular N3 algorithm [Sled 1998]
- iterative method for bias field estimation using:
 - B-spline approximation
 - multi-resolution
 - masks, weight image



Improved Bias Field Correction using N4ITK

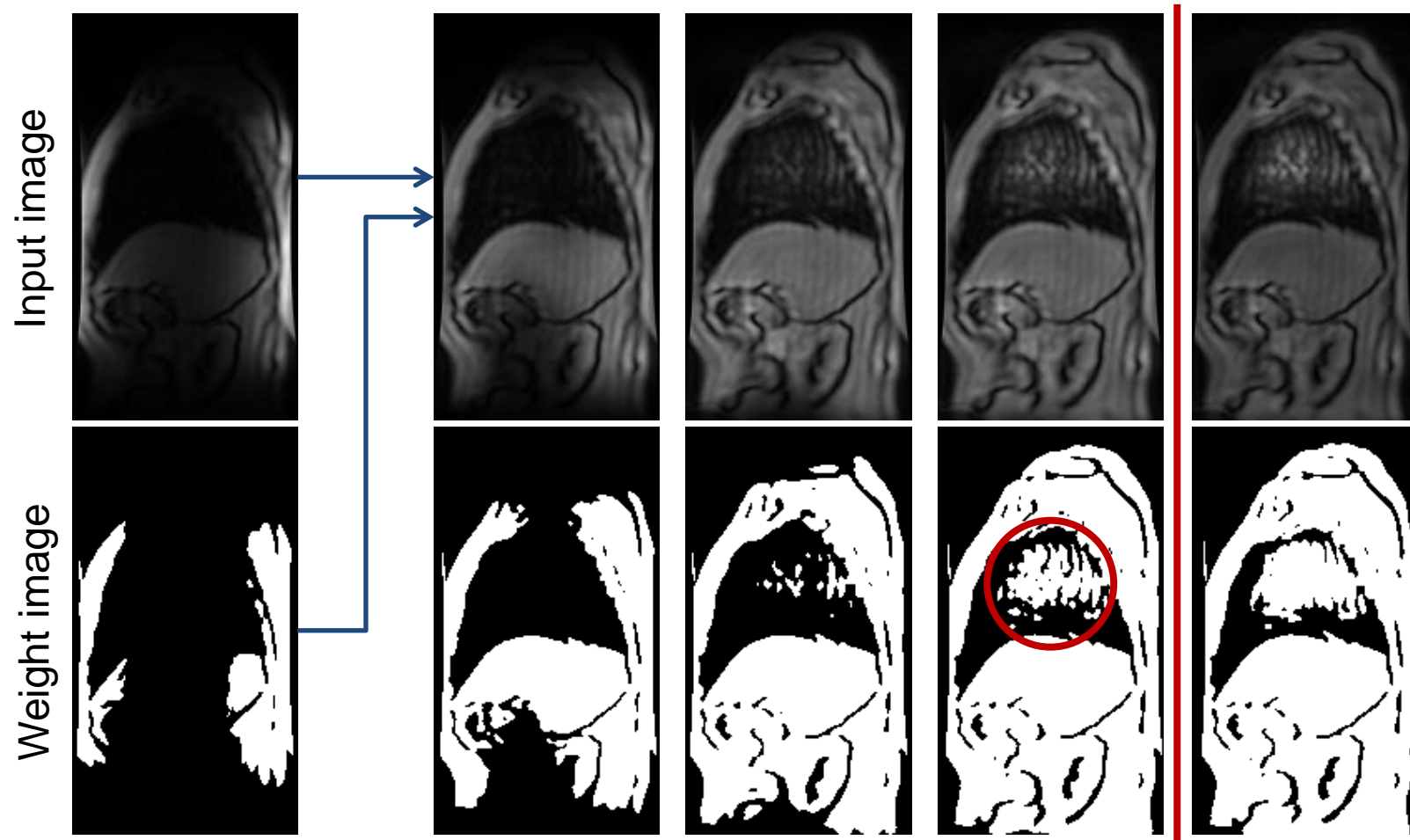
Parameter optimization

- spline distance
- number of resolutions
- number of iterations per resolution
- weight image

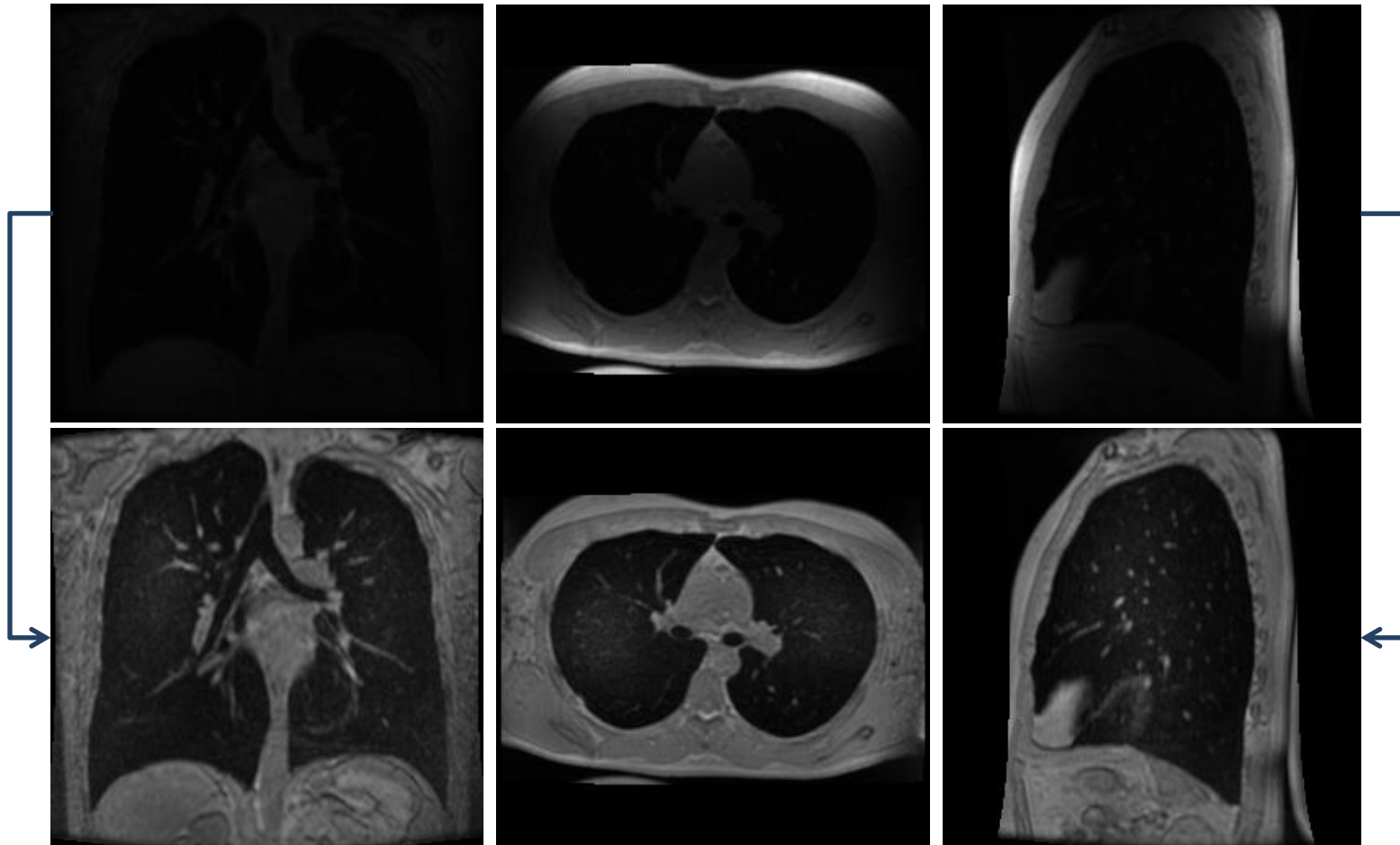
Iterative procedure:

- multiple runs of N4ITK on original image
- create mask from previous run via Otsu thresholding of the result

Improved Bias Field Correction using N4ITK

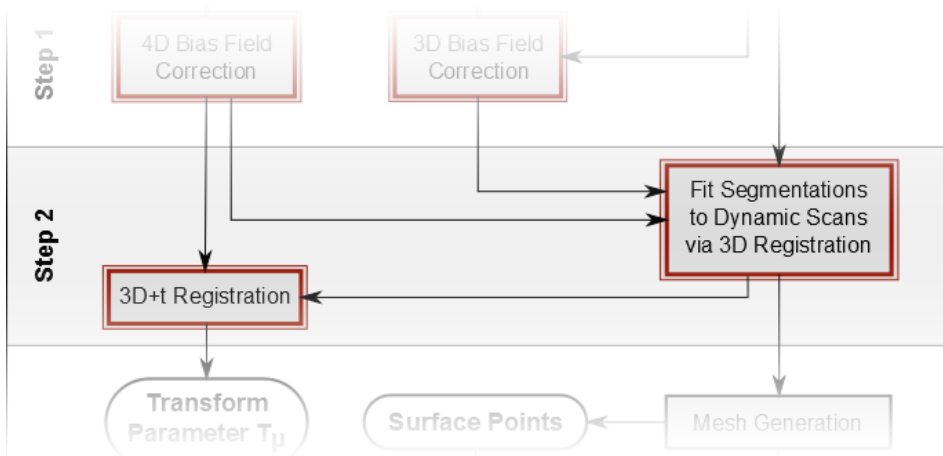


Improved Bias Field Correction using N4ITK





Respiratory Motion Estimation



Non-rigid Registration of 3D+t Images

Main components [Metz 2011]

- transformation: free-form B-spline deformation model
- metric: variance of intensity values over time
- multi-resolution strategy

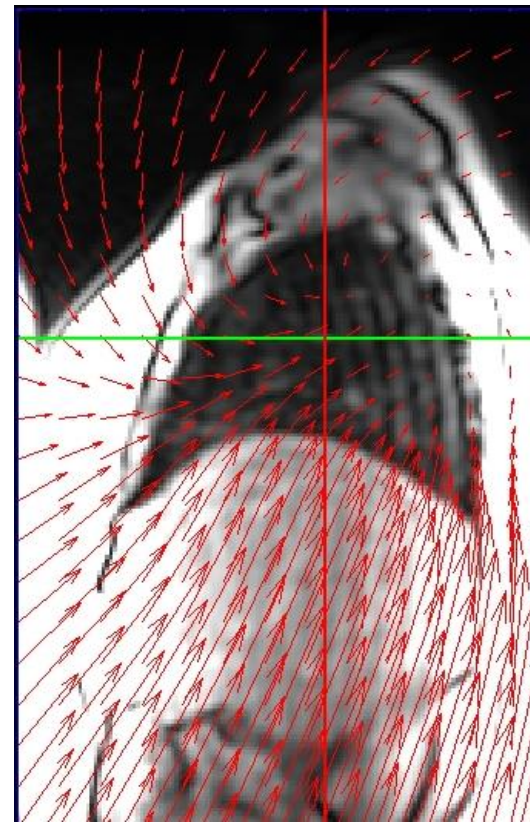


Parameter optimization

- spline distance forward transformation
- spline distance inverse transformation

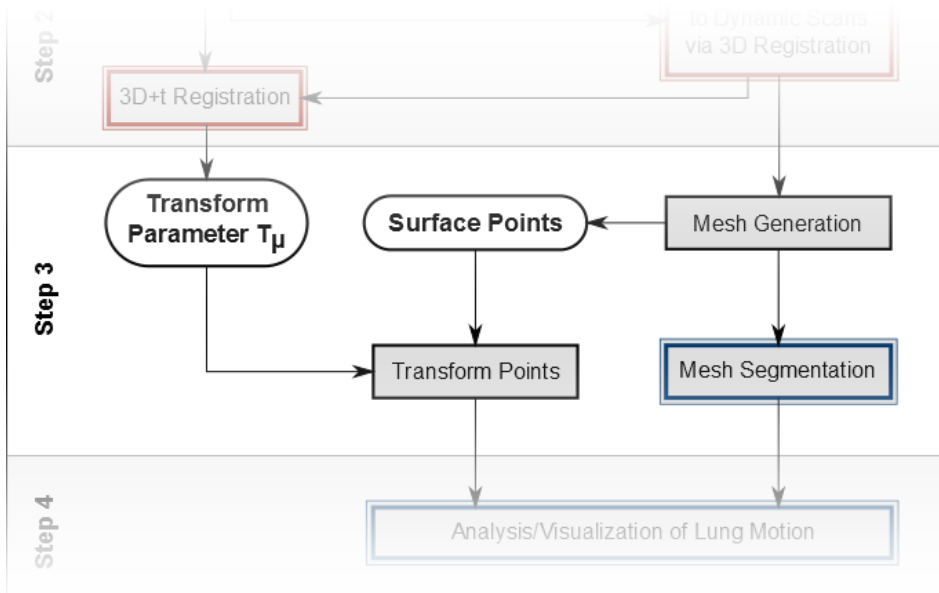
Non-rigid Registration of 3D+t Images

Dense deformation field calculated from transformation parameters





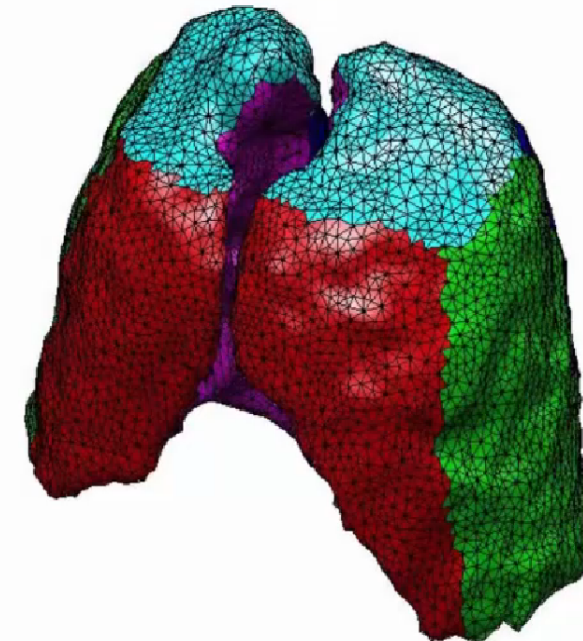
Lung Partitioning



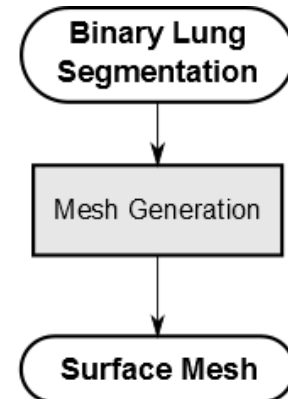
Lung Surfaces

Partitions of the lung surface

- base (diaphragmatic surface)
- mediastinal surface
- costal surface
 - anterior
 - posterior
 - lateral
 - apex



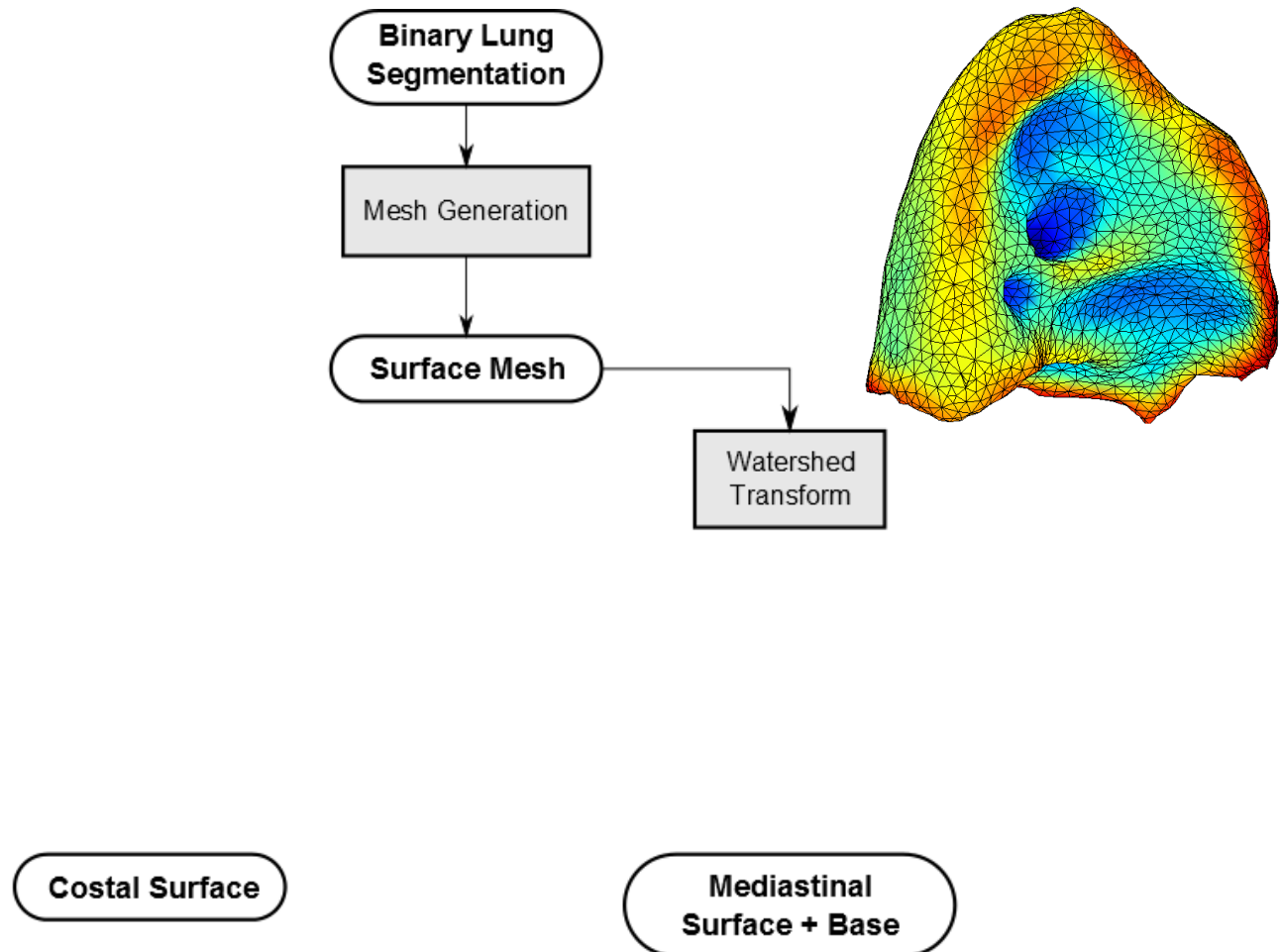
Mesh Segmentation Pipeline



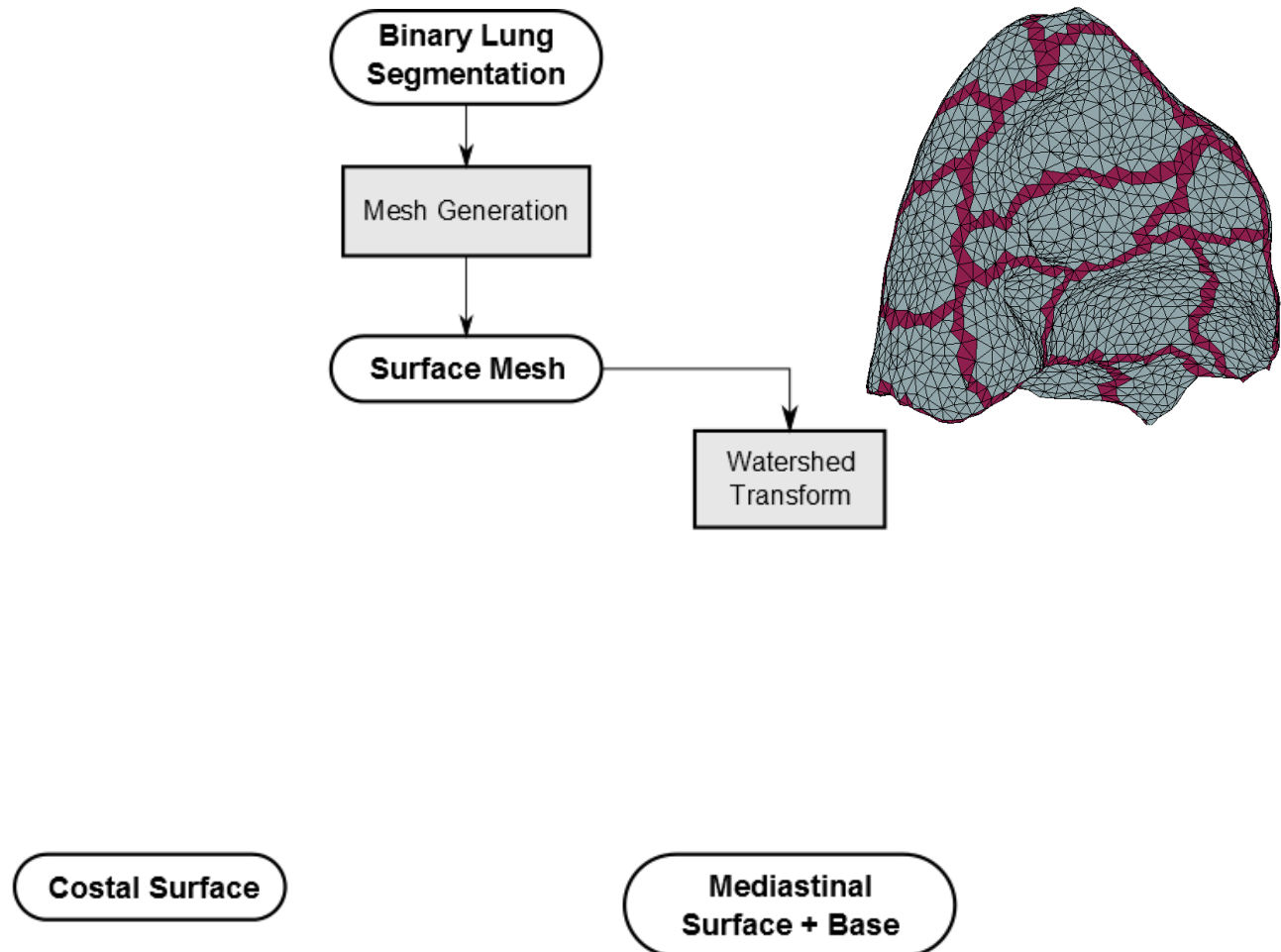
Costal Surface

**Mediastinal
Surface + Base**

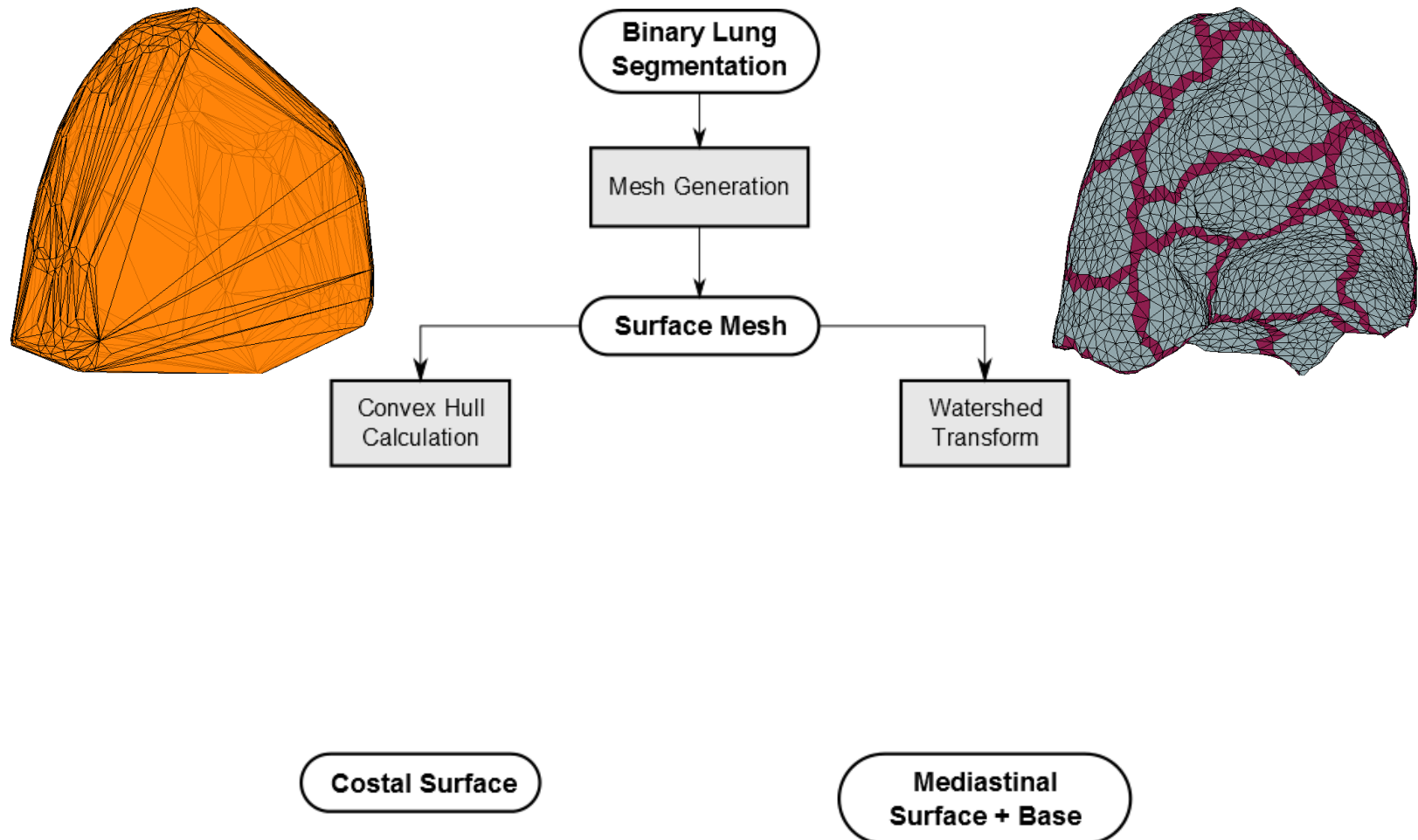
Mesh Segmentation Pipeline



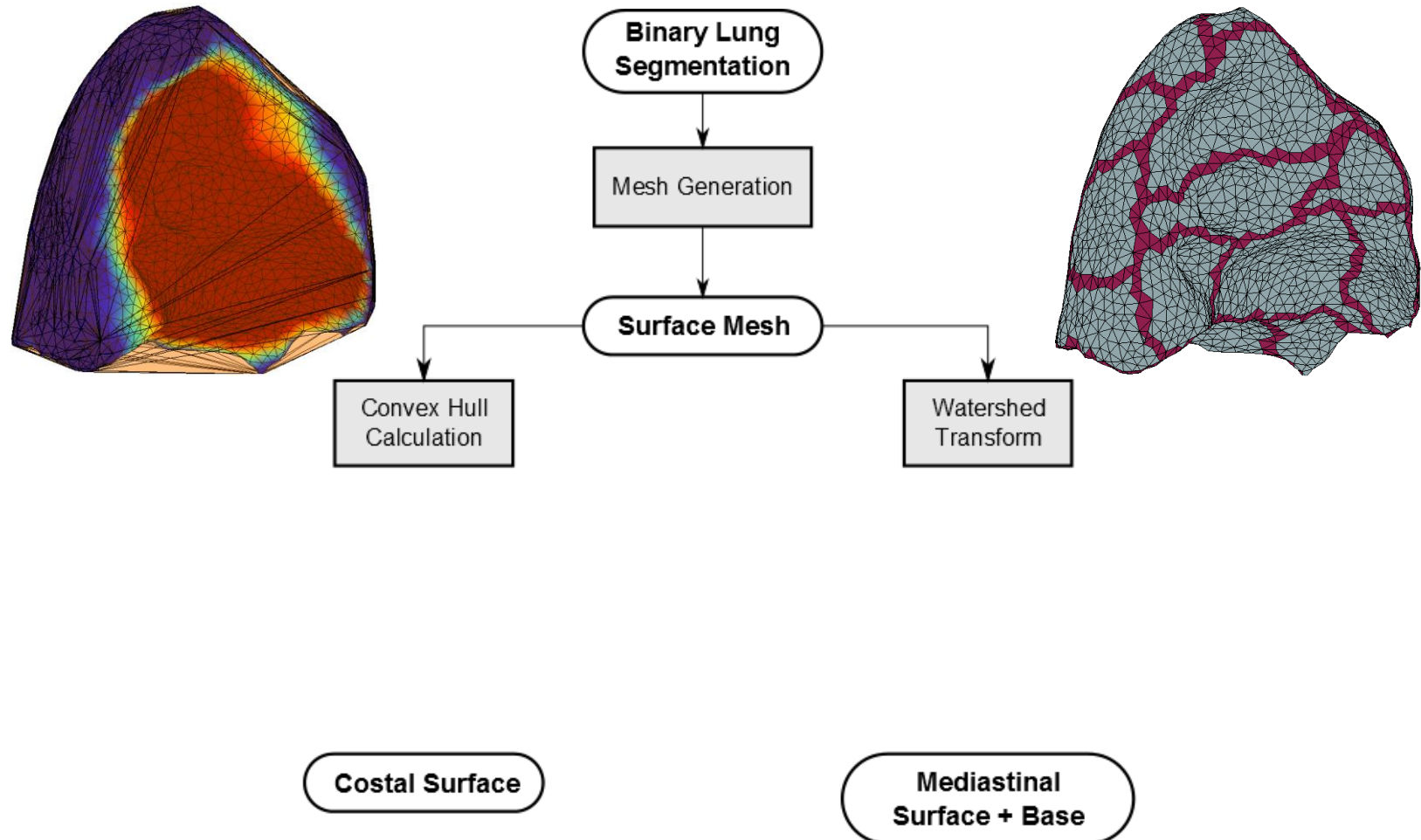
Mesh Segmentation Pipeline



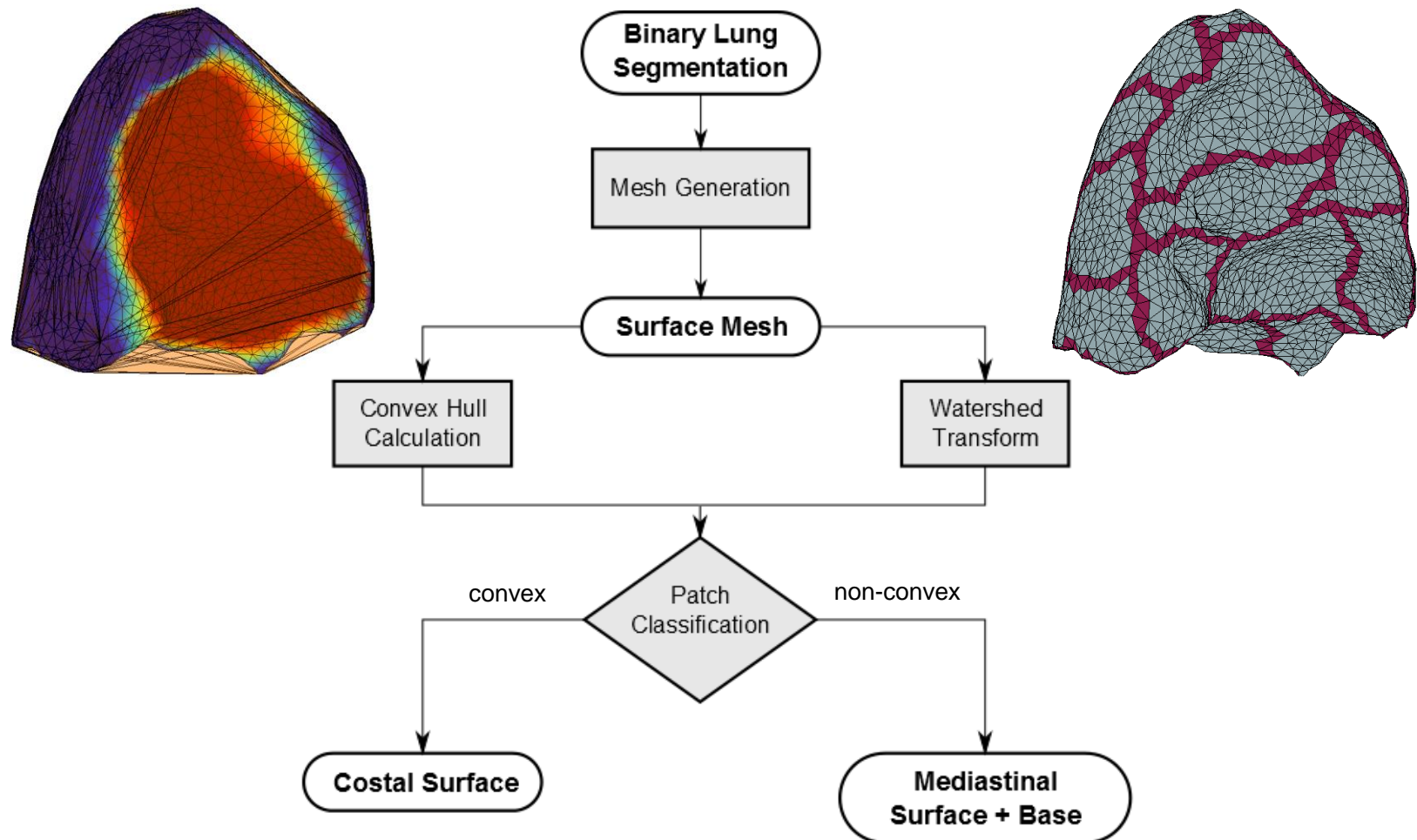
Mesh Segmentation Pipeline



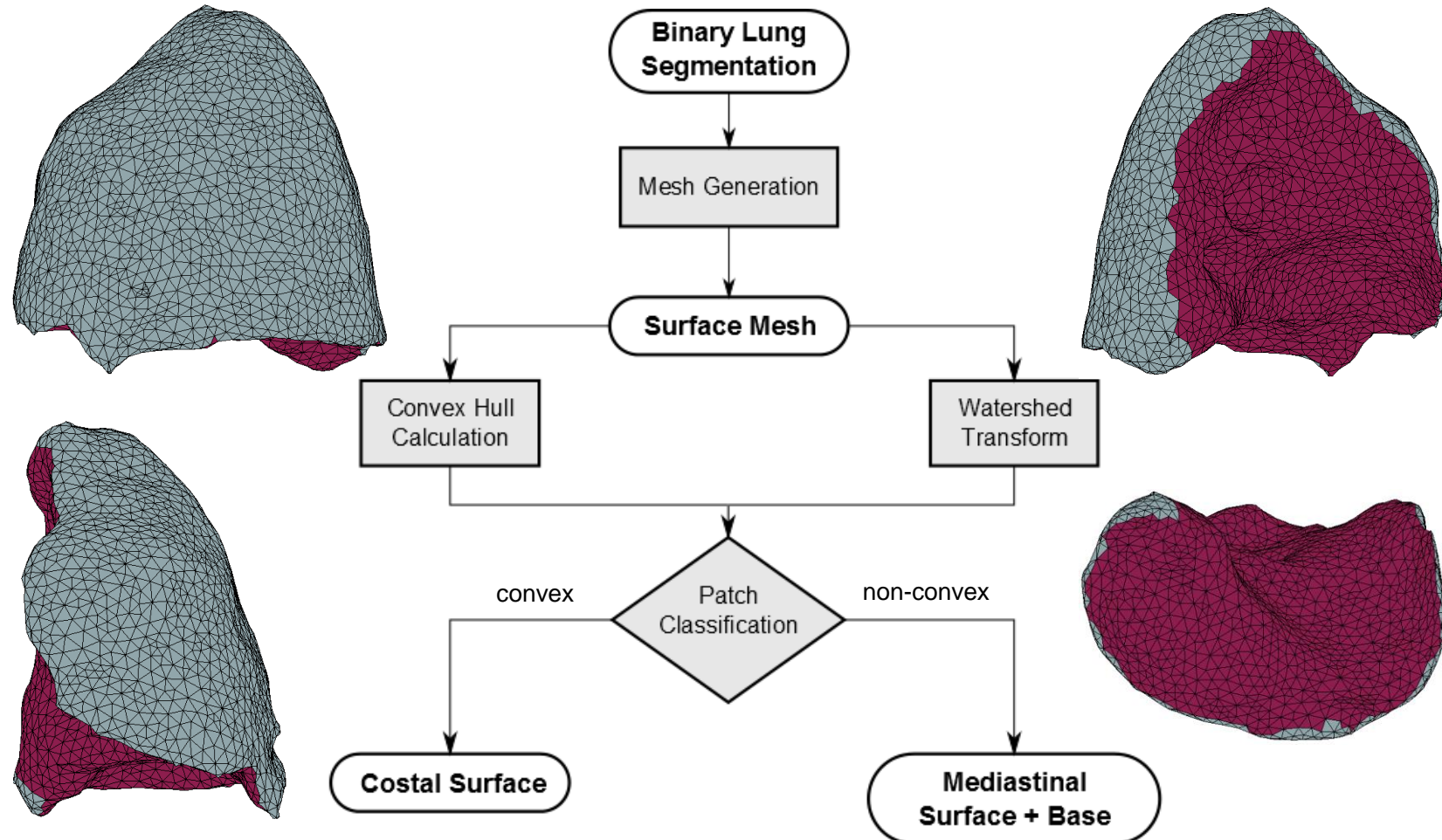
Mesh Segmentation Pipeline



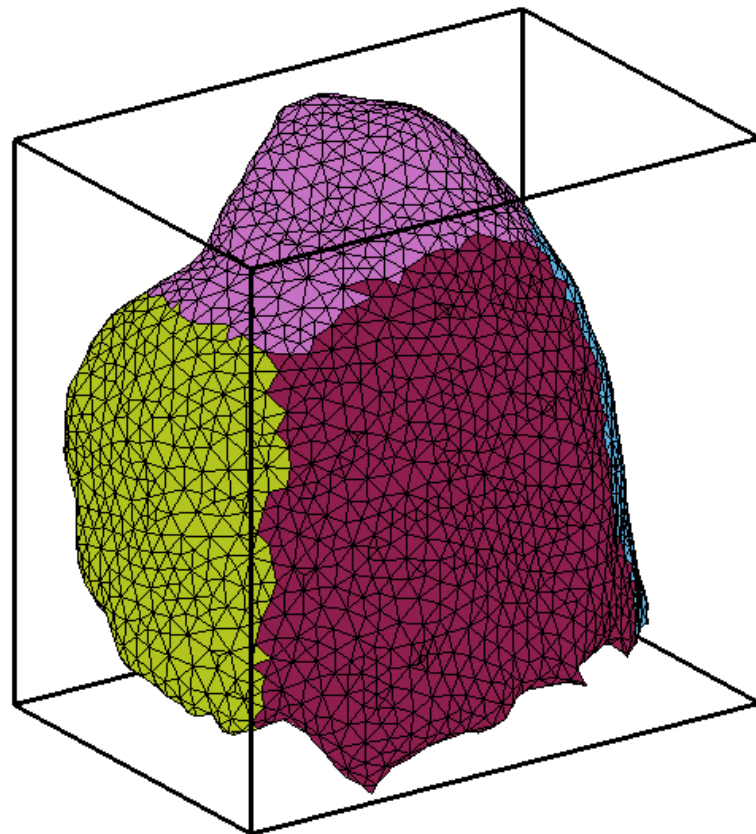
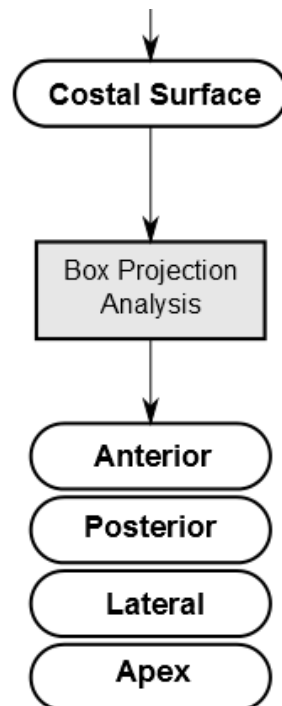
Mesh Segmentation Pipeline



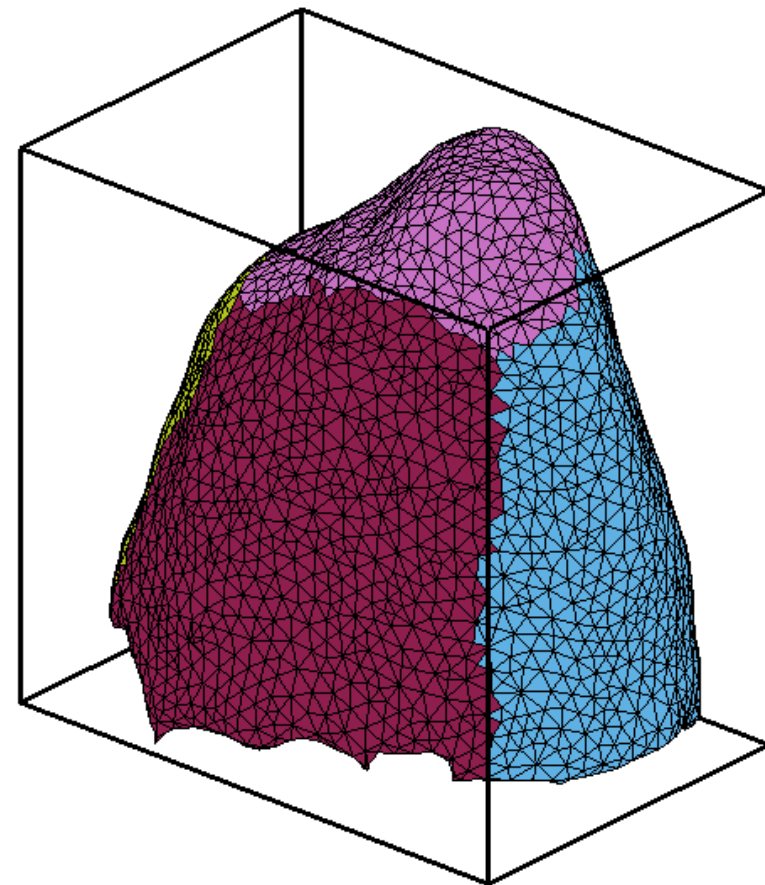
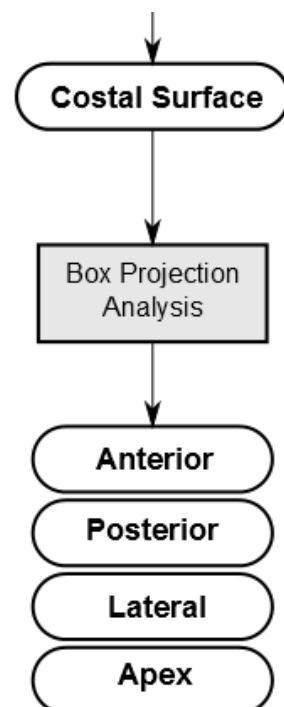
Mesh Segmentation Pipeline



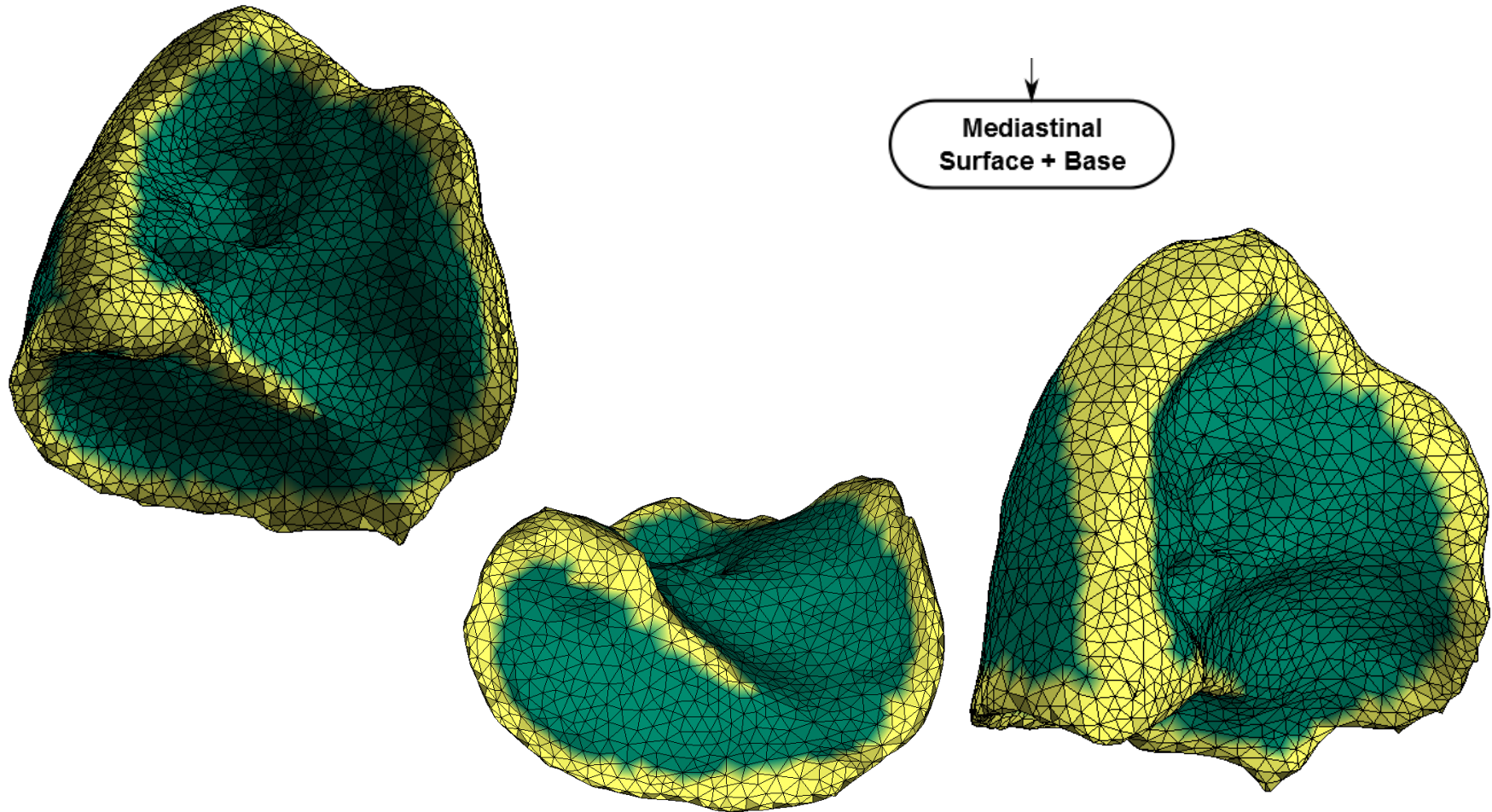
Mesh Segmentation Pipeline



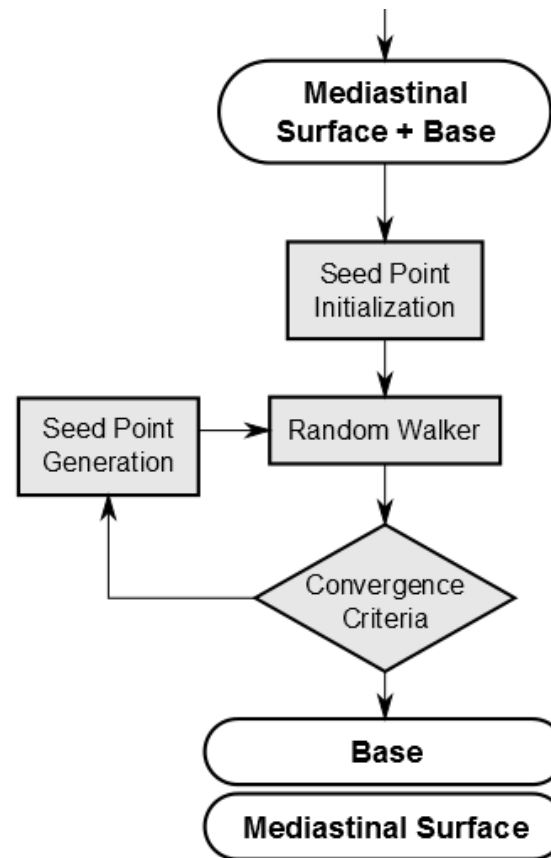
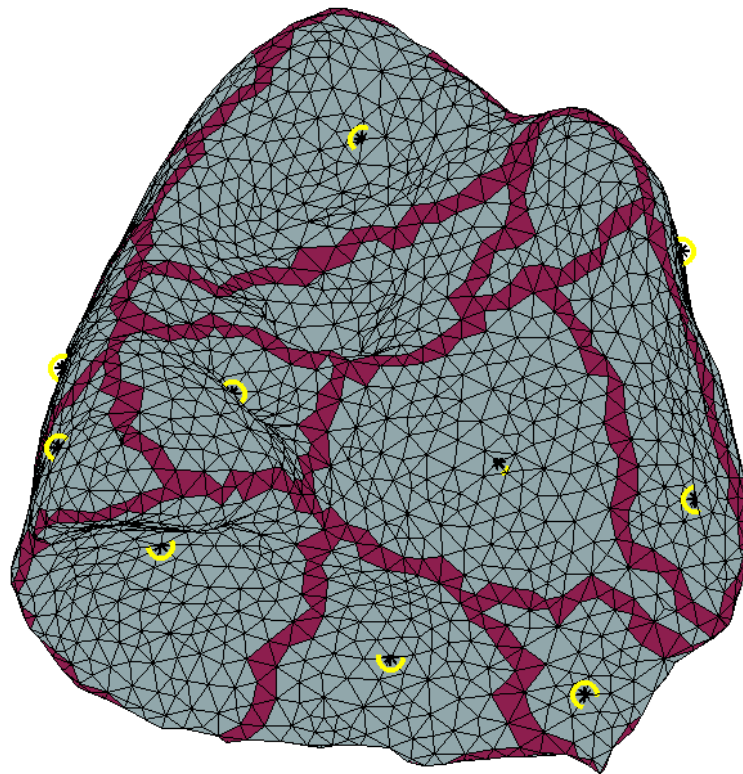
Mesh Segmentation Pipeline



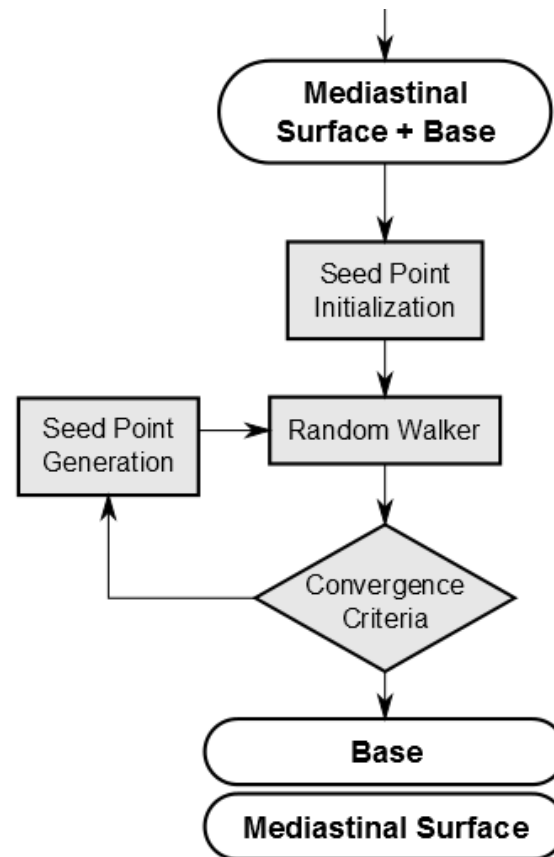
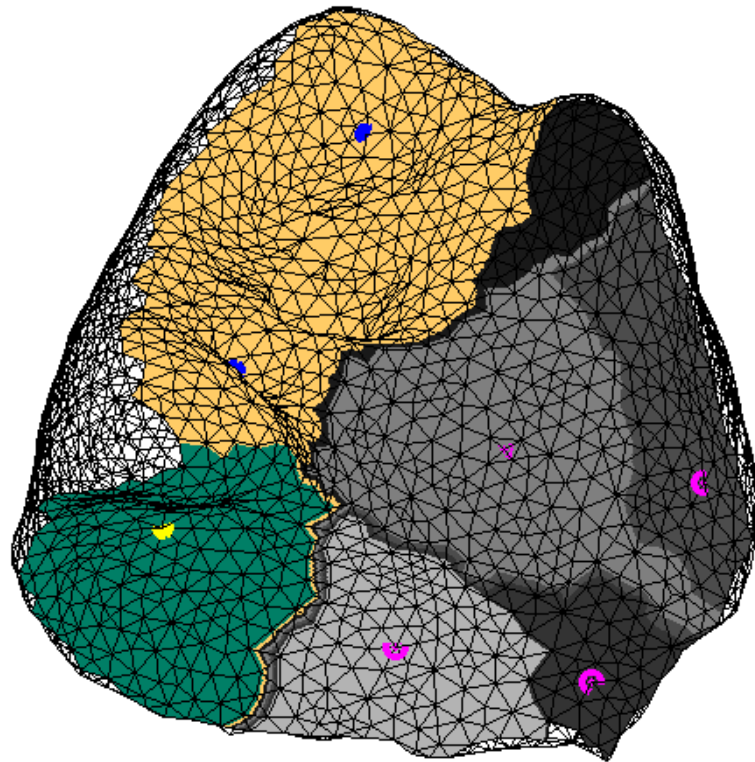
Mesh Segmentation Pipeline



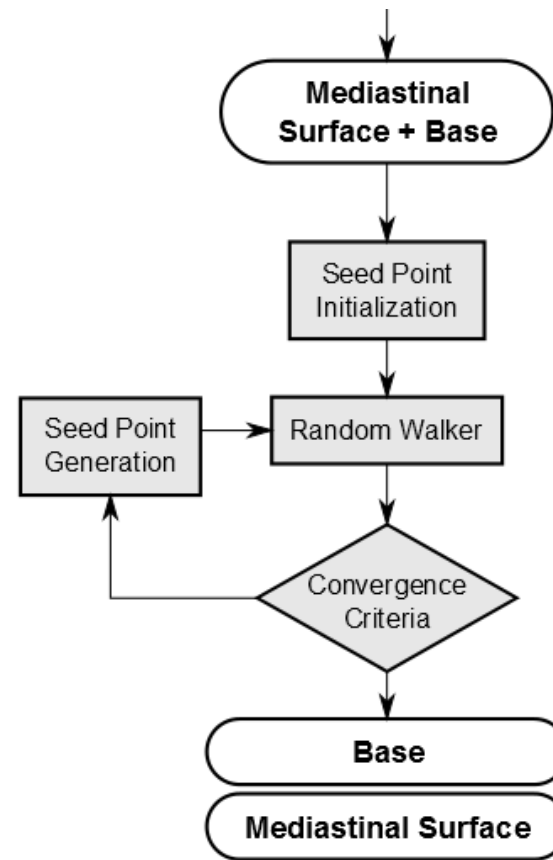
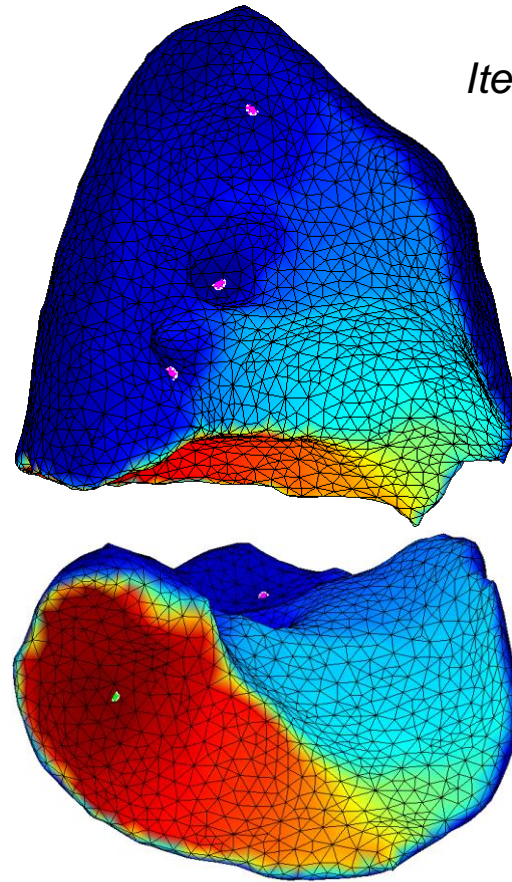
Mesh Segmentation Pipeline



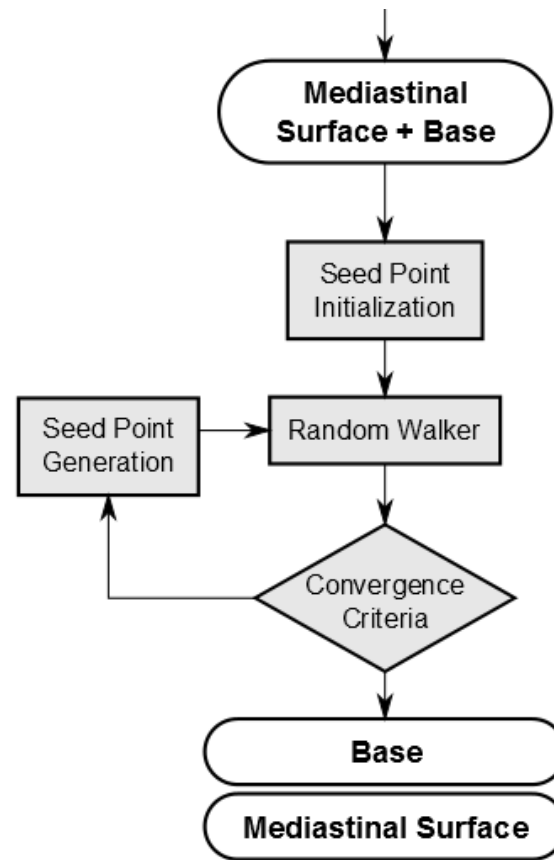
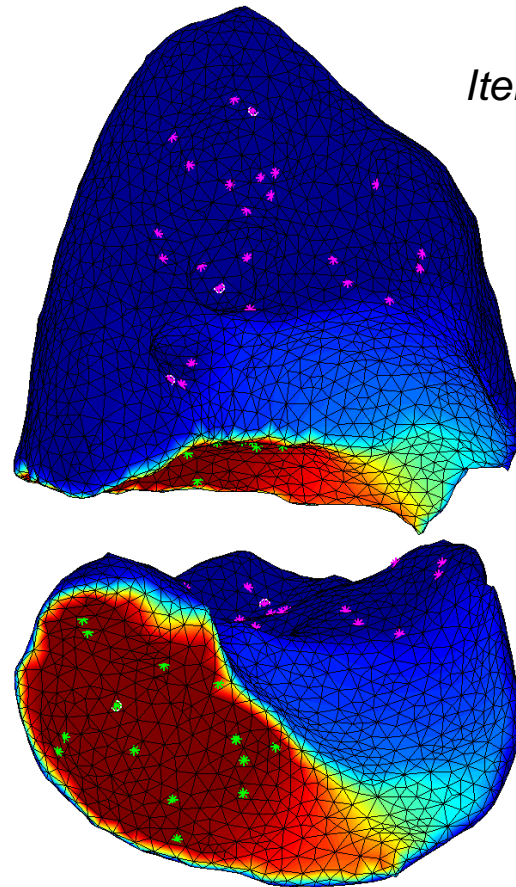
Mesh Segmentation Pipeline



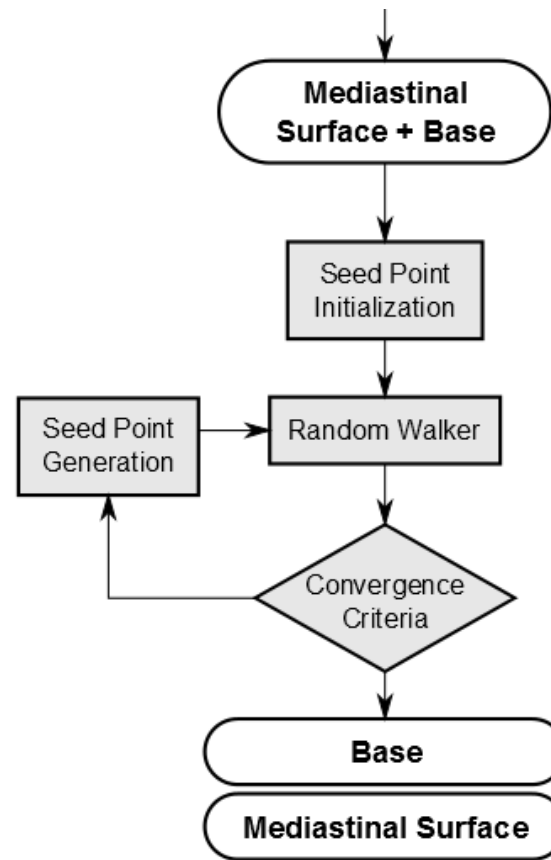
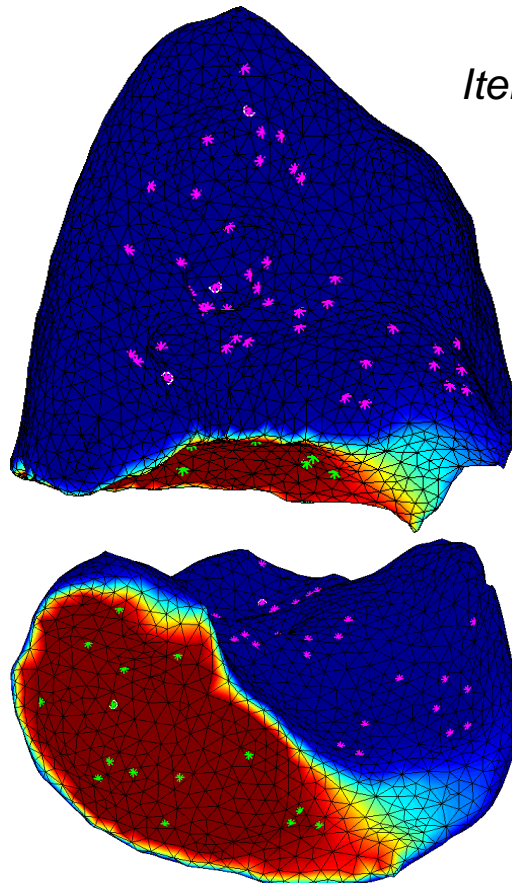
Mesh Segmentation Pipeline



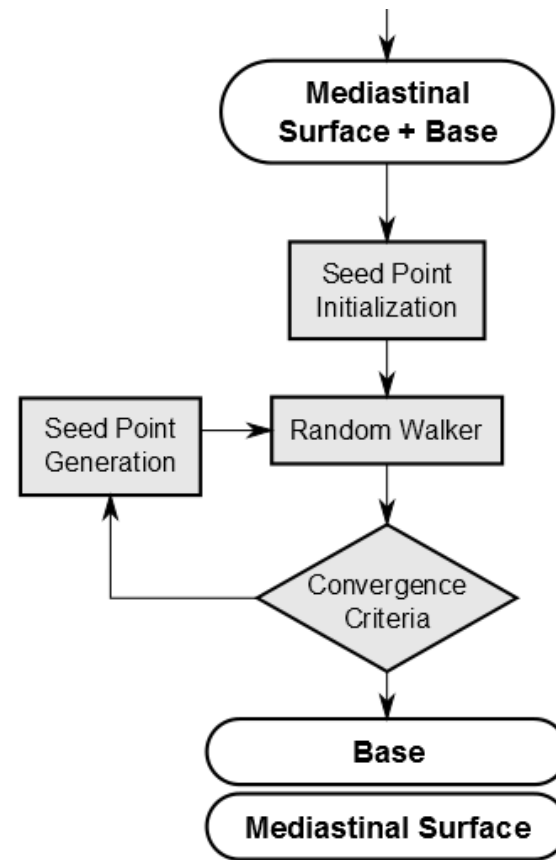
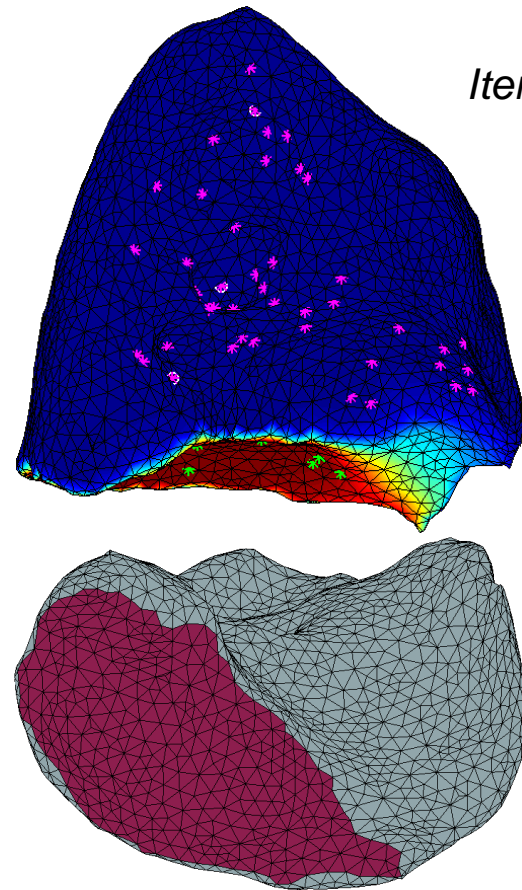
Mesh Segmentation Pipeline



Mesh Segmentation Pipeline

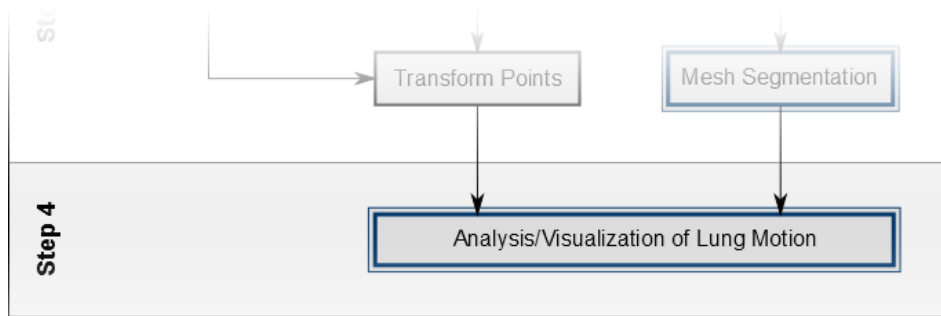


Mesh Segmentation Pipeline





Motion Feature Extraction



Global Motion Features

Lung **volume** calculated from mesh

Lung **size** in sagittal plane

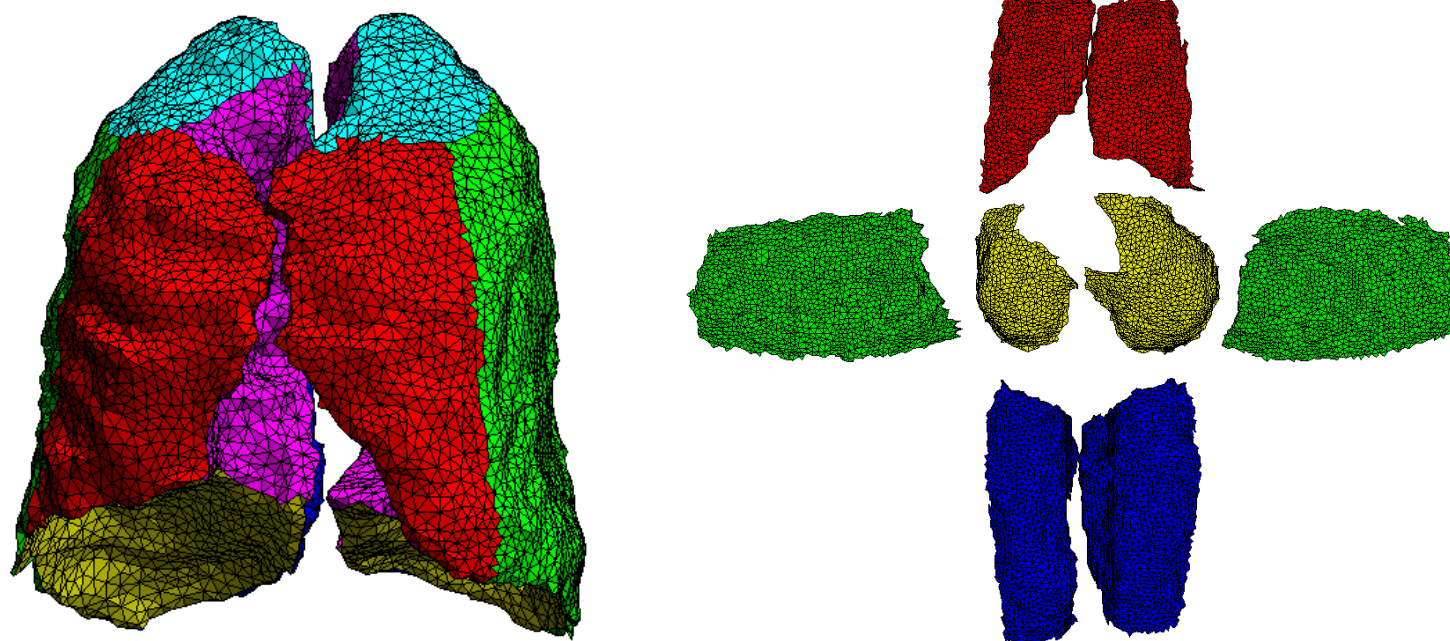
- anteroposterior size: front most to back most point
- craniocaudal size: highest point of base to highest point apex

(Optional) differentiation between left and right lung

- **expected behavior is not present in all cases**
- **local analysis necessary**

Local Motion Features

- extract feature per vertex
- for easy visualization unfold lung based on segmentation



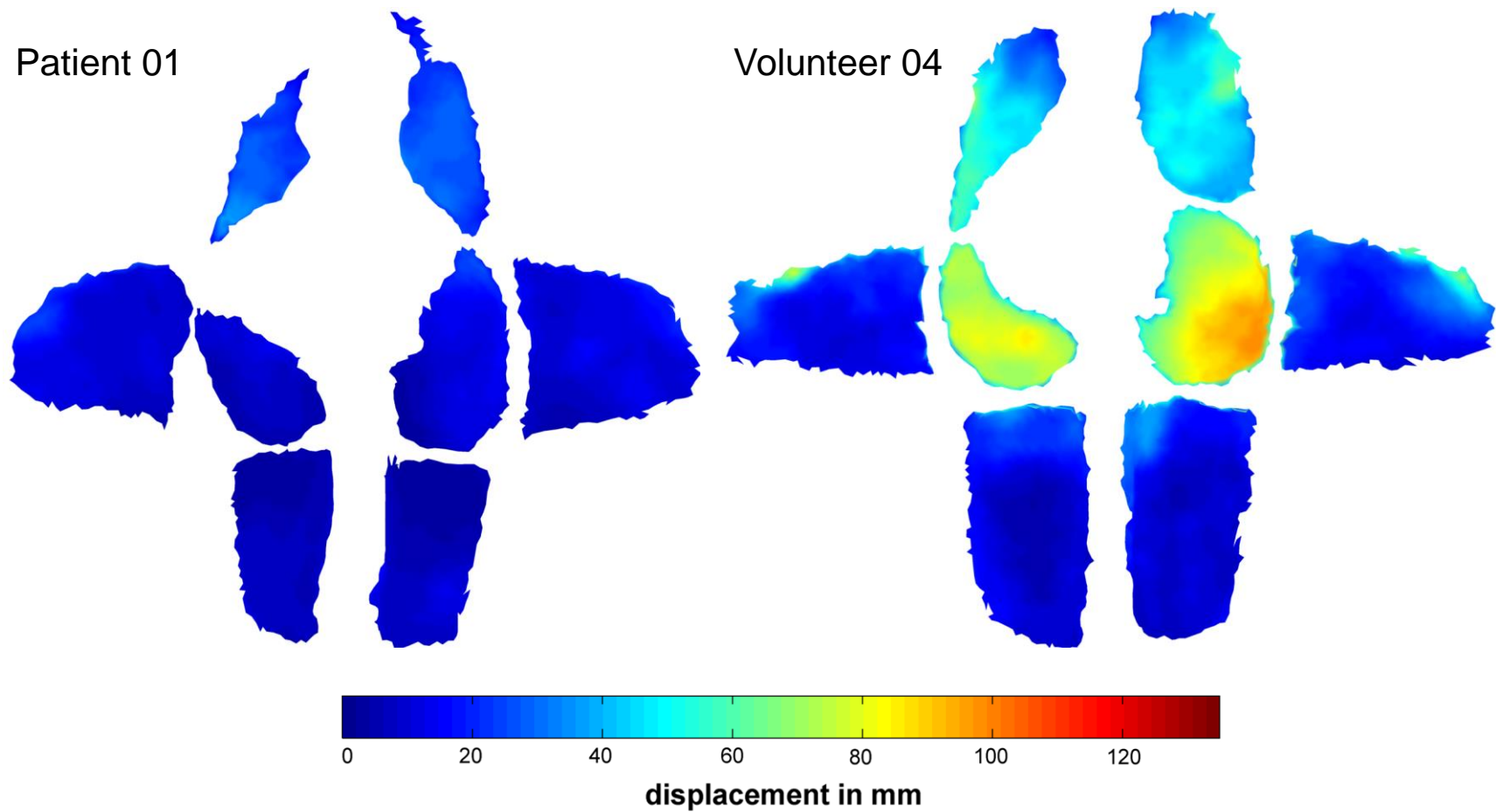
Local Motion Features

Total path length

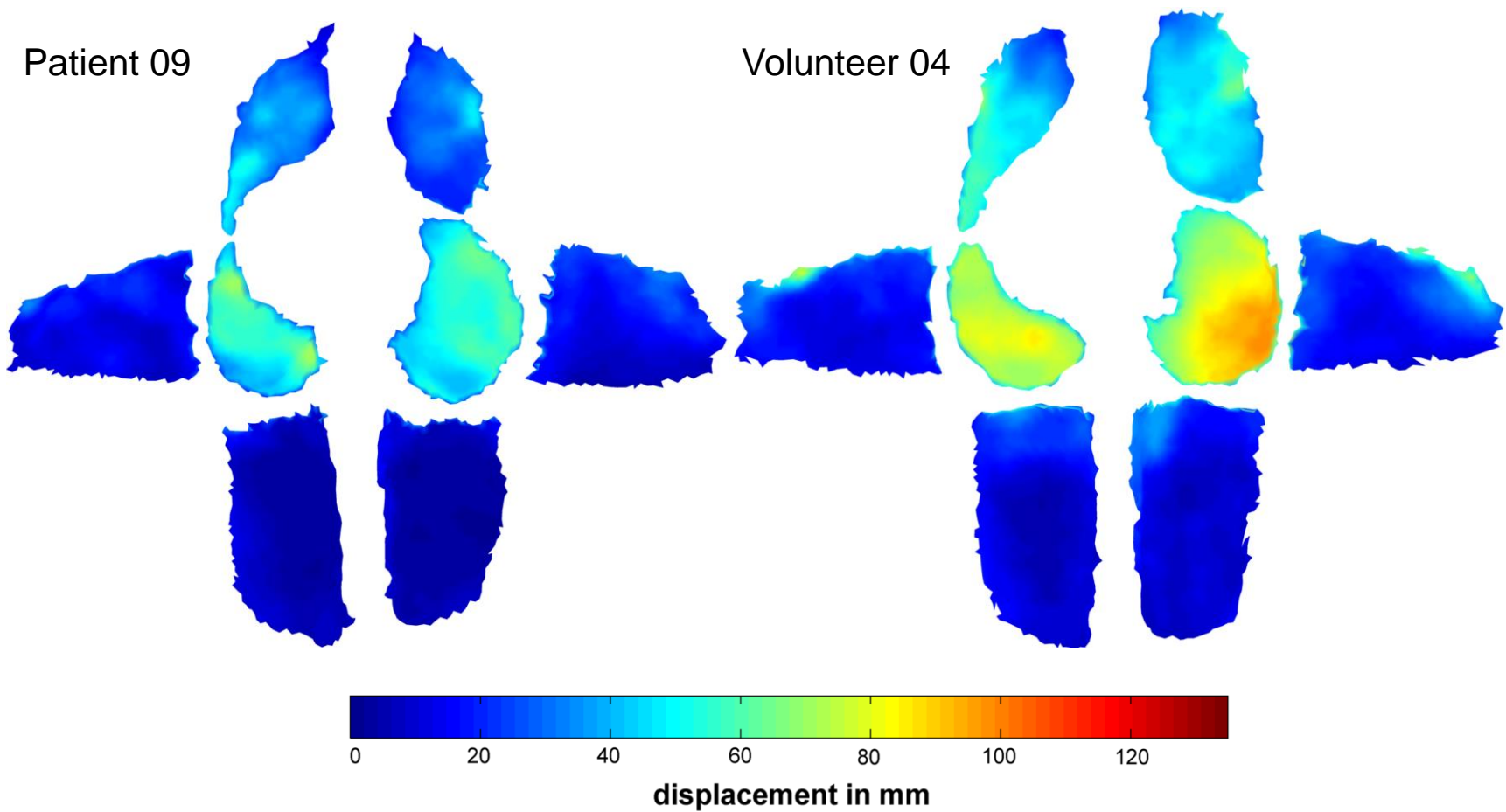
Total displacement

- **in direction related to segment**
- in axial plane
- in craniocaudal direction

Local Motion Features



Local Motion Features





Conclusion and Outlook

Conclusion

Main steps have been taken towards a full automatic framework for lung motion characterization

- image preprocessing via bias field correction
- registration of dynamic sequence for estimation of lung deformation
- lung surface partitioning
- global and local motion analysis related to respiratory muscles

Results have high relevance for clinicians

Personal conclusion: in practice it is a very long way from the medical images provided by a radiologist to the aimed final quantitative analysis

Outlook

- automatic lung segmentation
- improvement of registration to handle ghosting
- analysis of other breathing maneuvers
- analysis of more patients and volunteers to build reference standard
- build ground truth for better optimization and evaluation

References

- Kondo, T., et al. (2000). A dynamic analysis of chest wall motions with MRI in healthy young subjects. *Respirology*, 5(1), 19–25.
- Naish, J., Revest, P., & Court, D. S. (2009). *Medical Sciences* (1st ed., pp. 702–704). Edinburgh, UK: Saunders/Elsevier.
- Gauthier, A., et al. (1994). Three-dimensional reconstruction of the in vivo human diaphragm shape at different lung volumes. *Journal of Applied Physiology*, 76(2), 495–506.
- Plathow, C., et al (2009). Estimation of pulmonary motion in healthy subjects and patients with intrathoracic tumors using 3D-dynamic MRI: initial results. *Korean Journal of Radiology*, 10(6), 559–567.
- Heimann, T., et al. (2007). A shape-guided deformable model with evolutionary algorithm initialization for 3D soft tissue segmentation. *Information Processing in Medical Imaging*, 20, 1–12.

References

- Sled, J. G., et al. (1998). A Nonparametric Method for Automatic Correction of Intensity Nonuniformity in MRI Data. *IEEE Transactions on Medical Imaging*, 17(1), 87–97.
- Tustison, N. J., Avants, B. B., Cook, P. A., Zheng, Y., Egan, A., Yushkevich, P. A., & Gee, J. C. (2010). N4ITK: Improved N3 Bias Correction. *IEEE Transactions on Medical Imaging*, 29(6), 1310–1320.
- Metz, C. T., et al. (2011). Nonrigid registration of dynamic medical imaging data using nD + t B-splines and a groupwise optimization approach. *Medical Image Analysis*, 15(2), 238–249.
- Grady, L. (2006). Random walks for image segmentation. *IEEE Transactions on Pattern Analysis and Machine Intelligence*, 28, 1768–1783.

Figures

- Fig. 1: MasterScreen Pneumo Spirometer (<http://www.carefusion.com>)
- Fig. 2: Diaphragm (Gray's Anatomy for Students)
- Fig. 3: Breathing mechanics (OpenStax College. The Process of Breathing, OpenStax-CNX Web site. <http://cnx.org/content/m46549/1.6/>, Jun 28, 2013.)
- Fig. 4: Diaphragm movement (Gauthier et al. 1994)
- Fig. 5: Lung deformation (Plathow et al. 2009)



Thank you for your attention!

